Major and trace elements in suspended matter of western Siberian rivers: First assessment across permafrost zones and landscape parameters of watersheds

Ivan V. Krickov, Artem G. Lim, Rinat M. Manasypov, Sergey V. Loiko, Sergey N. Vorobyev, Vladimir P. Shevchenko, Olga M. Dara, Vyacheslav V. Gordeev, Oleg S. Pokrovsky

Major and trace elements in suspended matter of western Siberian rivers: first assessment across permafrost zones and landscape parameters of watersheds

Ivan V. KRICKOV[1], Artem G. LIM[1], Rinat M. MANASYPOV[1,2], Sergey V. LOIKO[1], Sergey N. VOROBYEV[1], Vladimir P. SHEVCHENKO[3], Olga M. DARA[3], Vyacheslav V. GORDEEV[3], Oleg S. POKROVSKY[1,2,4*]

[1] *BIO-GEO-CLIM Laboratory, Tomsk State University, Tomsk, Russia*
[2] *Institute of Ecological Problems of the North, N. Laverov Federal Center for Integrated Arctic Research, Arkhangelsk, Russian Academy of Science, Russia*
[3] *Shirshov Institute of Oceanology, Russian Academy of Science, Moscow, Russia*
[4] *Geosciences and Environment Toulouse, UMR 5563 CNRS, 14 Avenue Edouard Belin 31400 Toulouse, France*

**Email: oleg.pokrovsky@get.omp.eu*

Key words: trace metals, toxicant, micronutrient, season, river suspended matter, permafrost, Siberia

Submitted to *Geochim. Cosmochim. Acta,* after revision October 2019

Abstract

In contrast to good understanding of chemical composition of the river suspended matter (RSM) of large rivers, small rivers remain strongly understudied, despite the fact that they can provide valuable information on mechanisms of RSM generation and transport depending on key environmental parameters of the watershed. This is especially true for permafrost-affected boreal and subarctic territories, subjected to strong modification due to permafrost thaw and landscape changes under climate warming. We selected Earth's largest frozen peatland zone, the western Siberia Lowland (WSL) in order to test an impact of climate warming, permafrost thaw and landscape zone changes on riverine transport of particulate material from mainland to the Arctic Ocean. We sampled 33 small and medium size WSL rivers during spring flood, summer baseflow and autumn flood over a 1700 km gradient of climate and permafrost. Major and trace elements in particulate (> 0.45 μm) and dissolved (< 0.45 μm) fraction were analyzed. We hypothesize that future increase in active layer thickness and the change of dominant landscape from bogs and lakes to forest can be predicted via analyzing the actual pattern of RSM chemical composition across various permafrost zones and landscape parameters of WSL river watershed. We observed a minimum concentration of Li, Mg, Na, K, Rb, V, Cr, Zn, Cu, Co, Ni, Al, Ga, Y, REEs, Nb, W, Ti, Zr, Hf, Th and U in RSM collected from isolated and sporadic permafrost zones. Considering all seasons together, the presence of forest in the permafrost-bearing zone increased particulate concentrations of all alkalis and alkaline-earth elements, B, As, Nb, Mn, Co, Al, Ga, REEs, Ti, Zr, Hf, Th. This is consistent with element mobilization from mineral horizons that become available for interacting with soil fluids under forested regions. Lakes retained particulate alkaline-earths, Fe, Mn, Co, trivalent and tetravalent hydrolysates (TE^{3+}, TE^{4+}). The concentration of lithogenic low-soluble elements (TE^{3+}, TE^{4+}) in the RSM strongly increased with the river size (watershed area).

Compared to the world RSM average, the WSL rivers exhibited lower concentrations of all elements except Mn and P and a low share of suspended elements relative to total

(suspended+dissolved) forms of trace metals and of low-mobility (lithogenic) elements. Likely reasons for these features are: *i*) low runoff and low RSM concentration as there is no rock and mineral substrate exposed to physical weathering in WSL peatland; *ii*) organic, rather than mineral, nature of surrounding "solid" substrates and as a result, organic rather than silicate nature of RSM, and *iii*) high DOC and Fe concentration leading to high concentrations of typically low-solubilty elements in the dissolved (< 0.45 μm) fraction due to colloids.

From a climate warming perspective, the increase in active layer thickness and involvement of mineral horizons into soil fluid migration in discontinuous to continuous permafrost zone will likely increase the share of particulate fraction in total element transport for many soluble (labile) elements and also lithogenic elements in WSL rivers. At the same time, permafrost boundary shift northward may decrease particulate concentrations of most major and TE in rivers of discontinuous permafrost zone. The lake drainage and forest colonization of tundra and bogs in the permafrost-affected part of WSL may increase the concentration of alkali and alkaline-earth elements, divalent metals and trivalent and tetravalent hydrolysates. As a result, export of particulate metal micronutrients and toxicants from the WSL territory to the Arctic Ocean may increase.

1. Introduction

The change of export of major and trace element, including macro- and micro-nutrients, from the land to the ocean in high latitude regions under various climate change scenarios is among the major scientific challenges of aquatic biogeochemistry (Hobbie et al., 1999; Holmes et al., 2000; Guo et al., 2004; Heinze et al., 2015; Toohey et al., 2016). The overwhelming number of studies in high latitudes dealt with dissolved rather than particulate fraction of the river load (Holmes et al., 2000; Cooper et al., 2008; Vonk et al., 2015; Tank et al., 2016; Kaiser et al., 2017), despite the fact that the majority of continental runoff to the ocean occurs in particulate rather than dissolved form (Meybeck, 1982; Schlesinger and Melack, 1981; Gislason

et al., 2006; Viers et al., 2009; Gordeev and Lisitzin, 2014). In contrast to numerous studies that have been devoted to the biogeochemistry of "dissolved" organic carbon and macro-nutrients in large rivers of the circumpolar zone (Gordeev, 2000; Lobbes et al., 2000; Stedmon et al., 2011; McClelland et al., 2016; Guo et al., 2004; Tank et al., 2012b, 2016; O'Donnell et al., 2016; Kaiser et al., 2017; Drake et al., 2018), very few works characterized major and trace elements other than C and nutrients in the particulate (> 0.22 or 0.45 μm) fraction. Gordeev et al. (1996) and later Nikanorov et al. (2010) and Magritsky (2010) compiled the data from the Russian Hydrological Survey on suspended load of Arctic rivers, but no data for chemical composition was available. Gebhardt et al (2004) provided extensive data set for RSM concentration, C and N composition in the mixing zone of the Ob and Yenisey Rivers. Occasional data on elementary composition of RSM in boreal and subarctic rivers are available for European part of Russia (Morozov et al., 1974; Shevchenko et al., 2010; Savenko et al., 2004; Pokrovsky et al., 2010), Western Siberia (Gordeev et al., 2004), Central Siberian Plateau (Pokrovsky et al., 2015, 2016), Eastern Siberian Rivers (Kutscher et al., 2018), Canada (Gaillardet et al., 2003; Javed et al., 2018), the Mackenzie basin (Millot et al., 2010), and the 6 large Arctic rivers (data of PARTNERS and ARCTIC GRO; Holmes et al., 2002, 2012).

Moreover, one of the poorly studied aspects of RSM biogeochemistry is the impact of watershed size because small rivers remain strongly understudied in terms of their suspended load (Holmes et al., 2002). The reason for this is that, in anthropogenically-affected regions, the small rivers are subjected to strong modification by human activity; thus, the natural signal of RSM chemistry in these rivers is strongly blurred and does not allow assessment of mechanisms for suspended load formation. In pristine regions, the small rivers are hardly accessible because the human population and all field logistics are linked to large rivers. In addition to the paucity of data on RSM from small and medium-size rivers, there is another bias of seasonal aspect on RSM transfer by rivers: most available data represent easily collectable (dissolved) fraction of the river load, often sampled during summer baseflow on large rivers. This bias is especially

pronounced in high latitude boreal regions where the largest share of suspended flux occurs during spring freshet period, but the access to these sites during the full hydrological year is highly limited.

In contrast to many other regions in the world, western Siberia allows to overcome these aforementioned natural obstacles with RSM sampling. This relatively pristine peatland has a unique geographical setting and a sufficiently developed road infrastructure. Interest in the Western Siberia Lowland (WSL), the largest permafrost-affected peatland area, stems from: *i*) its storage of a sizeable amount of C in thawed and frozen peat (Krementski et al., 2003), *ii*) the fact that it is a significant reservoir of dissolved organic carbon in surface water (Polishchuk et al., 2017, 2018), *iii*) the fact that it supplies a large amount of freshwater and solutes to the Arctic Ocean (Frey et al., 2007a, b; Frappart et al. 2010), and *iv*) its emissions of high fluxes of greenhouse gases from the water area of bogs, lakes and rivers to the atmosphere (Shirokova et al., 2013; Sabrekov et al., 2017; Serikova et al., 2018, 2019). The permafrost in WSL is highly unstable and thaws faster than in other Siberian regions (Romanovsky et al., 2010). Due to the high fragility of permafrost in western Siberia, climate change is likely to have a profound influence on the magnitude of riverine fluxes through alteration of hydrological regimes in WSL rivers (Frey and McClelland 2009; Bring et al. 2016) and stimulation of element releases caused by widespread permafrost thawing (Vonk et al. 2015).

An important gap in our knowledge of RSM geochemistry is the role of landscape features of the watersheds, such as forest and bog coverage, as well as permafrost distribution. This information can be acquired from a sufficient number of small watersheds (i.e., < 10,000 km²) that cover a wide range of climate and physico-geographical zones on otherwise similar lithology. Among all global boreal and high latitude regions, only WSL offers possibility for testing the impact of landscape parameters and climatic conditions on RSM in rivers of various sizes that drain highly homogeneous rock substrates (peat overlaying silts and sands). Such a unique geographical situation of the WSL allows foreseeing the impacts of climate warming,

permafrost thaw and forest line migration to the north via analyzing ecosystem parameters across a climate and permafrost gradient at otherwise similar lithological and geomorphological environments. Such a substituting of "space for time" approach has been successfully used in western Siberia for the dissolved (< 0.45 μm) fraction of inorganic river load (Frey et al., 2007b), DOC (Frey and Smith, 2005; Pokrovsky et al., 2015), trace metals (Pokrovsky et al., 2016) and nutrients (Frey et al., 2007a; Vorobyev et al., 2017). On a broader context, this approach postulates that contemporary spatial phenomena can be used to understand and model temporal processes that are otherwise unobservable such as past and future events (Blois et al., 2013).

In this work, we studied chemical composition (major and trace elements) of RSM collected in small, medium and large rivers over 3 main hydrological seasons in the world's largest frozen peatland. Within the substituting space for time scenario, that is well established in this part of Siberia, we hypothesized that the a) permafrost boundary shift northward, b) increase in the active (unfrozen) layer thickness (ALT) and drainage of lakes, and c) transformation of bogs into forest that are anticipated within climate warmings scenarios can all be approximated via comparing the current status of RSM geochemistry across rivers that drain various landscapes and permafrost zones. Specifically, we expected that thickening of the active layer and colonization of palsa bogs by forest would enhance the involvement of mineral horizons in particulate flux from the soil profile to the river via suprapermafrost flow. Alternatively, the disappearance of permafrost should bring about more active participation of underlying silt and sand deposits into RSM flux formation in both small and large rivers. The present work is aimed at testing these hypotheses via conducting a primary survey of chemical composition for river particles across a sizable permafrost and climate gradient in western Siberia.

2. Sampling and analyses

2.1. Study site

We sampled 33 rivers that belong to the Ob, Pur and Taz watersheds in the Western Siberia Lowland (WSL). WSL is a huge peatland (> 2 million km²) situated across taiga forest, forest-tundra and tundra zones (**Fig. 1**). The position of these biomes follows a decrease in mean annual air temperature (MAAT) from -0.5°C in the south (Tomskaya region) to -9.5°C in the north (Yamburg). Annual precipitation ranges from 550 mm at the latitude of Tomsk, 650-700 mm at latitudes for Nojabrsk and Siberian Uvaly, and 600 mm at the lower reaches of the Taz River. The annual river runoff gradually increases northward, from 160-220 mm y^{-1} in the permafrost-free region to 280-320 mm y^{-1} in the Pur and Taz river basins which are located in the discontinuous to continuous permafrost zone (Nikitin and Zemtsov, 1986). Permafrost distribution also follows the same latitudinal gradient of MAAT changing from absent through isolated and sporadic in the south to discontinuous and continuous in the north. The landscape parameters of sampled catchments were determined by digitizing available soil, vegetation, lithological and geocryological maps (Pokrovsky et al., 2016; Vorobyev et al., 2017) as listed in **Table S1** of Supplementary Material. Sampling was performed during spring flood (17 May – 15 June 2016), summer baseflow (1 – 29 August 2016), and autumn baseflow before ice (24 September – 13 October 2016) and covered three main hydrological seasons. Note that the collected data set of suspended (> 0.45 µm) and dissolved (< 0.45 µm) WSL river load is unique and independent from previous studies of dissolved river load assessed during several seasons (2013-2015) in WSL (Pokrovsky et al., 2015, 2016). Our previous work in this region was devoted to the biogeochemistry of dissolved (< 0.45 µm) carbon and major and trace elements in rivers sampled over 4 main seasons in 2014 (February, June, August and October) (Pokrovsky et al. 2015, 2016), and dissolved nutrients sampled during Spring and Summer 2015 (Vorobyev et

198 al., 2017). Transport of the particulate suspended (> 0.45 µm) fraction of river load has not been
199 addressed before.

200 *2.2. Sampling of RSM*

201 During sampling we moved from south to north over a 2-3 week period collecting from
202 all rivers in the transect at approximately the same time after ice off and before ice on. To assess
203 inter-annual variations in RSM concentrations, we analyzed the RSM samples collected in WSL
204 rivers across the same transect during previous campaigns in spring 2014, 2015 and 2016 and
205 summer 2015 and 2016. Large water samples were collected from the middle of the river at 0.5
206 m depth in pre-cleaned polypropylene jars (30 to 50 L) and were allowed to decantate over 2-3
207 days. The water from the bottom layer of the barrels (approx. 30% of initial volume) was
208 centrifuged on-site for 20 min at 3500 rpm using 50-mL Nalgene tubes. Sediment was frozen at
209 -18°C and freeze-dried later in the laboratory. In addition to decantation and centrifugation, in
210 several rivers, the RSM was collected via direct filtration of large volumes (20 to 30 L) of river
211 water with an Inox (AISI 304) Teflon® PTFE-coated filtration unit (Fisher Bioblock) equipped
212 with 142 mm acetate cellulose Sartorius membranes (0.45 µm) and operated at 5-7 bars. An
213 average flow rate of 1-2 L/h was created by a peristaltic pump (MasterFlex B/T) with Teflon
214 tubing. The agreement in elementary composition of RSM between two methods of collection
215 was better than 20%. The total concentration of suspended material was determined in all
216 samples. For this, smaller volumes of freshly collected river water (1-2 L) were filtered on-site
217 (at the river bank or in the boat) with pre-weighted acetate cellulose filters (47 mm, 0.45 µm)
218 and Nalgene 250-mL polystyrene filtration units using a Mityvac® manual vacuum pump.
219

220 *2.3. Analyses*

221 Dissolved (< 0.45 µm) concentrations of major and trace elements in WSL river waters
222 were analyzed by ICP-MS as described elsewhere (Pokrovsky et al., 2016a, b). Major and trace
223 element concentrations in RSM collected from the large-volume separation procedure were

measured after full acid leaching in a clean room (class A 10,000) following ICP-MS (Agilent 7500 ce) analyses using methods for organic-rich natural samples employed in GET laboratory (Toulouse). The 100 mg dry weight powders were reacted for 30 min in an ultrasonic bath prior to full digestion using a Mars 5 microwave digestion system (CEM, France) using a mixture of 6.5 mL concentrated HNO_3, 3.5 mL concentrated HCl and 0.5 mL concentrated HF. HNO_3 and HCl were bi-distilled in the clean room and HF was of commercial ultra-pure quality (Fluka). For digestion, 10 samples of RSM, 1 certified 2711a Montana II Soil standard [or LKSD sediment] and 1 blank sample were loaded into Teflon reactors and were treated at 150°C for 20 min. After completing the digestion, contents of reactors were transferred into 30 mL Savilex vials and evaporated at 70°C. The residue was dissolved in 10 mL of 10% HNO_3 and diluted by 2% HNO_3 prior to analyses. The concentration of major and trace elements (TE) in filter digestion products was measured using an ICP-MS Agilent 7500ce with ~3 µg/L of In and Re as internal standards. Four in-house external standards were analyzed every 10 samples. The uncertainty for TE measurement ranged from 5 % at 0.1–100 µg/L to 10 % at 0.001–0.01 µg/L.

We interpreted the results for the elements that exhibited a good agreement between the certified or recommended values and our measurements within acceptable uncertainty levels ($([X]_{\text{recommended or certified}} - [X]_{\text{measured}}) / (([X]_{\text{recommended or certified}} + [X]_{\text{measured}})/2) \times 100 \leq 10\%$), or for cases in which we obtain a good reproducibility (the relative standard deviation of our various measurements of standards lower than 10%), even if no certified or recommended data are available. All certified major (Ca, Mg, K, Na) and trace element (Al, As, B, Ba, Co, Cr, Cu, Fe, Ga, Li, Mn, Mo, Ni, Pb), all REEs, Sb, Sr, Th, Ti, U, V, Zn) concentrations of the SLRS-5 standard (e.g., Yeghicheyan et al., 2013) and the measured concentrations agreed with an uncertainty of 10-20%. Agreement for Cd, Cs and Hf was between 30 and 50%. For all major and most trace elements, concentrations in blanks were below analytical detection limits (≤ 0.1-1 ng/L for Cd, Ba, Y, Zr, Nb, REE, Hf, Pb, Th, U; 1 ng/L for Ga, Ge, Rb, Sr, Sb; ≤10 ng/L for Ti, V, Cr, Mn, Fe, Co, Ni, Cu, Zn, As).

In addition to total chemical analysis after HF+HNO_3 digestion, 11 RSM samples of small, medium and large rivers collected in May and August were processed for total Si concentration using wet chemical analysis with photometric detection (see Gurvich et al., 1995; Baturin and Gordeev, 2019 for methodology). Further, the mineralogical composition of particulate fraction on selected filters was studied by X-ray powder diffractometric method on a D8 ADVANCE (Bruker AXS) X-ray diffractometer equipped with a LYNXEYE linear detector (Lisitzin et al., 2015). The uncertainty of the relative proportion of mineral composition was 1–2% and the detection limit was 1%. Due to limited amount of RSM available for analyses, the latter could be performed only on 3 rivers (small, medium and large one) sampled in May and August.

2.4. Statistical treatment

Statistical analysis was used to quantify the relationship between major and trace element concentrations in RSM and % of permafrost, amount of wetlands/lake/forest coverage in the watershed, and the surface area of the watershed ($S_{watershed}$). For simplicity, we distinguished five zones of permafrost distribution in river watersheds: 1) permafrost-free zones located south of 61°N latitude, 2) isolated zones located between 61 and 63.5°N latitude; 3) sporadic zones located between 63.5 and 65°N latitude; 4) discontinuous zones located between 65 and 66°N latitude, and 5) continuous permafrost zones located north of 66°N latitude. Non-parametric statistics were used because, based on Shapiro-Wilk test of the normality of variables, data on major and trace element concentrations in RSM and the fraction of particulate elements were not normally distributed. For these reasons, we used the median, 1st and 3rd quartiles, to trace dependence of nutrient concentrations to the type of permafrost distribution. Correlations between element concentration in RSM and main parameters of the watershed (latitude, watershed area, runoff, percentage of bogs, forest and lakes and the permafrost coverage) were tested using both Pearson and Spearman coefficients at $p < 0.05$ for permafrost-bearing and

permafrost-free zones during each season as well as all 3 seasons simultaneously. However, because the data were not normally distributed (as verified by the Shapiro-Wilk test of the normality of variables) and due to the small number of samples in the permafrost-free zone (N=8) and possibly non-linear relationships, we preferably presented Spearman's rank correlation coefficient in Results and Discussion below. Further, the Spearman coefficients provided generally better description of element concentration dependence on watershed parameters. The differences in suspended element concentration between different seasons and between each of the two adjacent permafrost zones were tested using a Mann-Whitney U test for a paired data set with significance level at 0.05. For unpaired data, a non-parametric H-criterion Kruskal-Wallis test was performed for all watershed sizes and all permafrost zones.

Multiple regressions were performed for quantifying the relationship between particulate concentration of TE and watershed parameters. More thorough statistical treatment of both log-transformed and non-transformed major and TE concentration in RSM included a normed principal component analysis (PCA). To identify groups of elements that behaved in a similar way in river water particles, we applied a complementary hierarchical cluster analysis (HCA) with the Ward's method for the linkages rule.

3. Results

For convenience, the elements were divided into 5 groups according to their basic physio-chemical properties, speciation in surface waters, affinity to colloids and dissolved organic matter, and behavior in peat soils of the region all of which were based on previous studies in WSL soils and waters (Stepanova et al., 2015; Raudina et al., 2017, 2018): 1) alkali and alkaline-earth metals, 2) oxyanions and neutral molecules (Si, B, V, Cr, Nb, W, As, Mo, Sb), 3) heavy metals (Fe, Mn, Cd, Pb, Zn, Cu, Co, Ni), 4) trivalent hydrolysates (Al, Ga, Y, REEs) and 5) tetravalent hydrolysates (Ti, Zr, Hf, Th).

The mineralogical composition of suspended matter (**Supplement A**) was strongly dominated by quartz (50-80%) and plagioclase (9-45%). The RSM of medium (Pyakopur, $S_{watershed}$ = 9881 km²) and large (Pur, $S_{watershed}$ = 112,000 km²) river exhibited small amount (< 10%) of K feldspar, amphibole, pyroxene, illite, chlorite and kaolinite which were however absent in small river (Vach-Yagun, $S_{watershed}$ = 99 km²). We could not find any systematic difference in mineralogical composition of RSM related to season (spring flood versus summer baseflow). Note that the RSM of all WSL rivers has unusually high concentration of organic carbon (15.3±9.7 wt.%) as averaged over seasons (Krickov et al., 2018). Small rivers ($S_{watershed}$ < 100 km²) have 2 to 3 times higher C_{org} (ca., 20-30%) compared to large ones (5-10% C_{org} in rivers with $S_{watershed}$ > 10,000 km²).

3.1. Element concentration in RSM as a function of watershed size, latitude, permafrost, and landscape parameters

The chemical composition of RSM across all seasons in WSL territory is provided in **Table 1**, whereas mean (± s.d.) concentrations during 3 seasons for each permafrost zone are listed in **Table S2**. Considering all seasons together, there was no significant difference (at $p < 0.05$) in element concentrations between permafrost-free and permafrost-bearing zone. The only exceptions are P, Ca, Mn, and Ba, which exhibited 2 x higher concentrations in the southern, permafrost-free rivers compared to northern rivers. The effect of permafrost type on major and TE in RSM is represented by box plots for the 5 groups of elements (**Fig. 2**). The overwhelming majority of elements yielded a U-shape dependence of RSM concentration on type of permafrost distribution. This dependence implied a minimum concentration in isolated to sporadic permafrost zone, and 3-5 times higher concentrations in permafrost-free and continuous permafrost zones compared to the beginning of permafrost disappearance (isolated and sporadic). These are elements in the 1st group (Li, Na, K, Rb, Mg), 2nd group (V, Cr, As, Nb, W, U), some elements of the 3rd group (Zn, Cu, Co, Ni), and all elements of the 4th and 5th groups

(TE^{3+}, TE^{4+}). As a result of this U-shape dependence of element concentration on the type of permafrost distribution, all the above mentioned elements exhibited a positive link to latitude and permafrost coverage in RSM of rivers draining through permafrost-bearing territories. Only a few elements did not follow this pattern: (*i*) Ca, Sr, and Ba were high in RSM of permafrost-free regions and demonstrated stable and low concentrations northward; (*ii*) B concentration increased northward, and (*iii*) Fe, Mn, Sb, Mo, Cd, Pb did not demonstrate any consistent (systematic) pattern for concentration dependence on type of permafrost.

Results of statistical treatment of watershed parameters (av. latitude, $S_{watershed}$, river runoff, % of bogs, forests, lakes and permafrost in the watershed) effect on element concentration in RSM (Spearman's rank correlation coefficient) are listed in Supplementary **Table S3** and analyzed below for separate groups of elements. Among the 1st group elements, alkali and Mg exhibited positive correlation with the watershed size ($R_{Spearman}$ = 0.5 to 0.9 in permafrost-free zone) during spring and summer. In the permafrost-bearing zone, the correlation was lower and became visible only in summer and autumn ($R_{Spearman}$ = 0.3 to 0.6). Latitude positively impacted all alkali and alkaline-earth elements in the permafrost-bearing zone during all three seasons. This is most likely linked to increase in these element concentration northward in the permafrost-bearing zone, as reflected in element box plots described above. In spring, lakes and bogs decreased the concentrations of Li, Na, K, Rb, Mg, Ca, Sr and Ba in the permafrost-bearing zone; this was also seen for Ca and Sr in summer and autumn. The effect of other watershed parameters on alkali and alkaline-earth element concentrations in RSM was not significant ($p < 0.05$). Among the 2nd group elements, V, Cr, Nb, and to a lesser degree W and U exhibited positive ($R_{Spearman}$ = 0.7 to 0.95) correlations with $S_{watershed}$ in permafrost-free regions in spring, summer and autumn. The effect however, was not pronounced in permafrost-bearing rivers. The concentrations of these elements in RSM were not affected by watershed landscape parameters. Statistical treatment of watershed size, permafrost, and landscape effect on Si concentration in RSM could not be performed due to low number of analyzed samples. There

353 was no clear relationship of Si with most environmental parameters of the watershed, except for
354 a local minimum at 20 to 30% permafrost coverage (**Supplement A**).

355 Neither the size of the watershed nor its landscape parameters strongly affected the
356 concentration of divalent 3rd group heavy metals. The exceptions are Ni and Cu, which positively
357 correlated with watershed size in permafrost-free zone in spring and summer ($0.70 < R_{Spearman} <$
358 0.93). Mn and Fe stand apart from other transition metals as their concentrations were generally
359 higher in small and medium watersheds ($S_{watershed} < 10{,}000$ km²) compared to larger ones (**Fig. 3**
360 **A, B**). Lakes exhibited a generally negative effect on Fe, Mn, and Co concentrations in the RSM
361 and bogs and lakes negatively affected Mn, Co, Ni and Zn concentrations in the RSM of the
362 permafrost-bearing zone during all seasons (**Table S3** and see **Fig. 3 C, D** as an example).

363 In the 4th and 5th groups, trivalent and tetravalent hydrolysates, $S_{watershed}$ significantly
364 increased ($p < 0.05$) concentrations of Cr, V, Al, Ga, Y, all REEs, Ti, Zr, Hf and Th in RSM.
365 This increase was mostly pronounced during summer and autumn (ca., a factor of 3 to 5 between
366 the rivers with $S_{watershed}$ = 10-100 km² and rivers with $S_{watershed} > 100{,}000$ km² as illustrated by
367 Al, Y, Ga, Ti, Zr, and Th in **Fig. 4 A, B, C, D, E and F**, respectively). Trivalent and tetravalent
368 hydrolysates were negatively impacted by the presence of bogs in the watershed, especially in
369 permafrost-bearing rivers (**Table S3**). Permafrost and latitude positively impacted the 5th group
370 (TE^{4+}) concentrations in RSM of rivers from the permafrost-bearing zone during all seasons.

371 Finally, we note that the inter-annual variations of major and TE concentrations for the
372 same 7 rivers sampled in 2014, 2015 and 2016 were generally not significant (Mann-Whitney
373 U-test $p > 0.05$). Several exceptions included Ti that was 20-30% lower in 2016 compared to
374 spring 2014/2015 and summer 2015; Mn, Fe, Co, Y, Mo, Cd and Ba (enriched in spring 2015
375 compared to 2016); and Co, Ge, Zr, Mo, Sb, Ce and Tl (enriched in summer 2015 over 2016).
376 However, most elements were not systematically different between years and further results are
377 focused on the most complete data set from 2016.
378

379 *3.2. Suspended over total (dissolved+suspended) fraction as a function of latitude and landscape*
380 *parameters*

381 The suspended fractions of all elements in WSL rivers averaged over all seasons and
382 permafrost zones are listed in **Table 2**. Depending on the mean value of suspended fraction, 3
383 major categories of elements in WSL rivers could be distinguished: (*i*) soluble, highly mobile
384 elements appearing < 20% in particulate form and > 80% in dissolved (< 0.45 µm) forms: Li, B,
385 Si, Na, Mg, K, Ca, Ni, As, Rb, Sr, Mo, Sb and Ba; (*ii*) insoluble elements transported essentially
386 (> 60%) in particulate forms: Al, Ti, Fe, Ga, Zr, Nb, Cs, REEs, Hf, Pb, Th, and (*iii*) other
387 elements present in both the particulate and soluble fraction (20 to 60%): V, Cr, Mn, Co, Cu, Zn,
388 Cd, Y, U. The first group included soluble, highly mobile alkalis, alkaline-earth and some
389 oxyanion elements. The second group included typical low mobility elements, which are usually
390 transported as particles rather than solutes. The third group included mainly transition metals that
391 were equally present in soluble and particulate form.

392 Soluble elements decreased the particulate fraction with increase in $S_{watershed}$ and
393 increased particulate fraction northward (as illustrated for Ca and Sr in **Fig. S1** of Supplement).
394 Fe was present essentially (> 50%) in particulate form with a lower fraction of RSM_{Fe} in small
395 watersheds (< 100 km²) compared to larger ones, and without clear relationship to bog, lake or
396 forest coverage in the watershed (**Fig. S2 A, B, C**). Mn exhibited lower particulate fraction in the
397 smallest rivers ($S_{watershed}$ < 100 km²) compared to large rivers (**Fig. S2 D**) and did not show any
398 significant linkage ($p > 0.05$) to latitude, permafrost or landscape parameters (not shown).

399 The share of suspended Al increased with the increase in $S_{watershed}$ and forest coverage
400 (**Fig. 5 A and B**, respectively). This effect was not observed for other insoluble elements such as
401 Fe and Mn. Ti, Zr and REEs also increased the particulate fraction with increase of the
402 watershed size (**Fig. 5 C, D** for Ti and Zr, respectively). Cu and Ni decreased the share of their
403 suspended transport with increase in forest proportion in the watershed (**Fig. S3 A, B**,

respectively), but increased with bog coverage (**Fig. S3 C, D**). Watershed size and latitude weakly affected Cu suspended fraction (**Fig. S3 E**) but did not influence Ni (not shown).

3.3. Multiparametric statistics

The PCA treatment of element concentrations in RSM and watershed physio-geographical parameters revealed two factors capable of describing only ~40% and 5-10% of overall variance. The F1 x F2 structure was highly similar and stable among seasons and permafrost zones for all rivers regardless of size. None of the factor were linked to landscape parameters. The 1st factor acted on most insoluble elements and divalent metals but also acted on alkalis and alkaline-earth metals. The 2nd factor acted on P, Ca, Sr, As, Ba, Mn and Fe (**Table S4, Fig. S4A**). It is important to note that 2nd factor was not pronounced in spring; during this high discharge period most elements (with exception of Mn, Sb, W) were controlled by the 1st factor and were merely linked to transport of silicate suspended material. The HCA yielded very strong links (linkage distance < 0.1) between insoluble elements (TE^{3+}, TE^{4+}) but also between some alkali and alkaline earth metals (Li, Na, Mg, K, Rb, Cs), V, and Ge. These alkali and alkaline earth metals were presumably hosted by silicate minerals (clays) dominating the RSM (**Table S4** and **Fig. S4 B**).

4. Discussion

We will begin by discussing the RSM concentration and its chemical composition compared to other rivers of N. Eurasia and more generally the world. We then transition into analyzing the impact of watershed size and seasons on variability of major and trace element particulate

concentrations across a latitudinal and permafrost gradient while also taking into consideration the function of landscape parameters on the watershed. We conclude with discussion on the possible impact of a permafrost boundary shift northward and change in proportion of landscape components (bogs, forest and lakes) on major and trace element concentrations in suspended material of WSL rivers.

4.1. Chemical composition of western Siberia river particles in comparison to world's rivers.

In general, the average chemical composition of RSM across the world is comparable to that of the upper part of continental earth crust or shale (Savenko et al., 2006a, b; Viers et al., 2009). Taking the average values of non-permafrost + permafrost zones as a whole for Western Siberia, we calculated the ratio of element concentration in the RSM of WSL to the average elementary concentration in suspended sediments of world rivers (Viers et al., 2009) as illustrated in **Fig. 6**. Typically, WSL rivers are impoverished (the ratio $0.2 \leq RSM_{WSL}/RSM_{World} \leq 0.5$) with respect to Mg, Al, K, Ca, V, Cr, Ni, Cu, Zn, Ga, Ge, Rb, Y, Cd, Sb, Cs, REEs, Tl, Th and U. Stronger depletion ($RSM_{WSL}/RSM_{World} < 0.2$) has been observed for Zr and Mo in WSL rivers. We interpret this result as being due to the sizeable proportion of organic matter in RSM in western Siberia (Krickov et al., 2018), and the corresponding impoverishment of suspended matter in elements hosted by silicate (clay) materials. Note however that the world average value is essentially based on data from big rivers. These rivers are enriched in silicate mineral-dominated components because they carry higher proportions of suspended silicate material and smaller fractions of organic-rich particles. The WSL rivers are sizebly enriched relative to the world average only with respect to P and Mn (a factor of 2.5 and 4.8, respectively). Along with elevated C concentration in suspended matter of WSL rivers (ca., 15%, Krickov et al., 2018), this reflects presence of peat particles and vegetation debris as important components of RSM. Further, WSL rivers contain sizeably amount of Mn^{2+} oxidation products which are supplied from surrounding lakes and bogs, leading to enrichment in Mn hydroxide. It is important to note

456 that certain pristine C-rich rivers in N. Europe (i.e. Kalix River) also demonstrate high Mn_{RSM}
457 concentrations due to formation of authigenic Mn oxides (i.e. Ponter et al., 1992; Andersson et
458 al., 1998). In western Siberia, the high enrichment of RSM in Mn during summer and autumn
459 may reflect biological removal of Mn^{2+} from lake and river water as well as immobilization of
460 dissolved Mn on the surface of phytoplankton due to local pH rise during photosynthesis. This is
461 consistent with laboratory microcosms (Shirokova et al., 2017) and the diurnal variation of Mn
462 concentration during phytoplankton bloom (Pokrovsky and Shirokova, 2013).

463 Another explanation for elevated Mn and P in WSL rivers is the origin of these elements
464 from an underground source. The 2nd PCA factor acted on Ca, Sr, Fe, Mn and P and was
465 pronounced only in summer and autumn, when the groundwater influx in the hyporheic zone is
466 highest. We hypothesize that anoxic conditions of the shallow groundwater create a favorable
467 environment for generation of P, Mn and Fe-enriched particles due to oxidation of Fe^{2+} and Mn^{2+}
468 and related to this P coprecipitation. However, the underground signal of Fe is offset (blurred) by
469 the high concentration of this element in riverine mineral particles originating from bank
470 abrasion and sedimentary rock physical weathering.

471 The REE upper-crust (UC) normalized pattern of average WSL rivers was rather flat with
472 only a slight Eu-Gd anomaly (**Fig. 7**). Similar flat patterns of REE distribution were reported for
473 many rivers across the world (Viers et al., 2009). In contrast to the majority of other rivers in the
474 world which exhibit stronger enrichment in REE relative to UC, WSL rivers are impoverished
475 compared to UC by a factor of ~2. Note that the lack of significant fractionation of REE in WSL
476 river particles is reflected in PCA and HCA diagrams showing compact clusters of all REEs. The
477 similarity of REE patterns in all WSL rivers and the lack of fractionation were presumably due
478 to highly homogeneous sedimentary rock substrate (silt and sand) dominating the WSL territory.
479 UC-normalized REE patterns for peat cores from WSL were also flat with Eu-Gd enrichment,
480 reflecting a crustal origin for solid and liquid aerosols incorporated by mosses and preserved in
481 the peat profile (Stepanova et al., 2015).

482

483 *4.2. Role of landscape factors and permafrost in elementary composition of RSM*

484 The present study allowed, for the first time in permafrost-affected territories, assessment
485 of the role of watershed size on chemical composition of RSM during different seasons.
486 Watershed size positively affected the concentration of many insoluble elements (TE^{3+}, TE^{4+}) in
487 the RSM (**Fig. 4, Table S3**). These elements are typically linked to a relatively dense and
488 insoluble (silicate) fraction of the suspended load. However, it is important to note that some
489 elements of the 1st group could be linked to clay minerals via ion exchange interlayer sites within
490 the clays. This is consistent with presence of illite and chlorite in RSM of large and medium size
491 rivers and the absence of these minerals in a smaller river (Supplement A, Table A2). The
492 positive link of $S_{watershed}$ to element concentrations in the RSM suggests that larger rivers have an
493 enhanced capacity for physical erosion of river bank and remobilization of riparian zone clay
494 sediments, especially pronounced during high flow. In contrast to large rivers, small rivers of the
495 WSL often flow within peat zones with relatively little access to water flux of mineral substrate
496 (Pokrovsky et al., 2015).

497 The forest coverage of the watershed was positively correlated with K, Rb, Sr, Mn, Co
498 concentrations in the RSM collected in spring (**Table S3**). Furthermore, considering all seasons
499 together, the presence of forest in the watershed positively acted on a number of elements but
500 only in the permafrost-bearing zone (**Table S3**). These are all alkalis and alkaline-earth
501 elements: B, As, Nb, Mn, Co, Al, Ga, REEs, Ti, Zr, Hf, Th. Such a long list of elements suggests
502 that the forest mobilizes not only organic litter but also mineral particles from the soil to the
503 river. This hypothesis is consistent with the following observations:
504 1) ALT strongly increases under forest growing in permafrost-affected territories of the WSL
505 (Goncharova et al., 2015), 2) soils under forest cover are mineral-rich podzols unlike organic-
506 rich histosols of palsa peat bog (Khrenov, 2011; Kulizhskiy et al., 2017a; Lim et al., 2017; Loiko
507 et al., 2017), 3) mineral soils under forest exhibit stronger biological activity compared to peat

508 soils (Goncharova et al., 2016), and 4) the removal of fine particles from soil occurs more
509 efficiently under well drained forest environment as it is known in various forest soils
510 (Tonkonogov, 1999; Quénard et al., 2011) including those of Western Siberia (Loiko et al.,
511 2015).

512 In reference to 1) the strong ALT increases under forests growing in permafrost-affected
513 territories of the WSL lead to preferential water discharge to rivers through subsurface and
514 shallow groundwater flow. This contrasts to shallow suprapermafrost flow within the peat
515 horizons in tundra and bog zones (Raudina et al., 2018). Or in other words, in forest settings,
516 thaw water flux over frozen horizons occurs through mineral layers in contrast to bog settings
517 where this water flows to the river through organic horizons. Deep water flow paths increase the
518 water travel time (Ala-aho et al., 2018) and lead to more efficient disintegration of mineral soil
519 particles before their delivery to the river. In reference to 2), since soils under forest cover are
520 mineral-rich podzols and not the organic-rich histosols of palsa peat bogs, forest soils are capable
521 of supplying a larger amount of mineral particles due to physical erosion of soil mineral
522 horizons. The potential of fine particles transport in some forest mineral soils of Western Siberia
523 has been recently demonstrated (Kulizhskii et al., 2017b). As such, forest soils may act as
524 sources for vertically and laterally moving C-rich colloids and suspensions. And finally in
525 reference to 3), stronger biological activity in mineral soils under forests (when compared to peat
526 soils) leads to stronger physical degradation of plant litter debris as well as mineral particles
527 during local transport within the soil profile.

528 A striking result of the present study is the minimum concentrations of most major and
529 TE in the sporadic to isolated permafrost zone belt (Li, Mg, K, Rb, V, Nb, U, Zn, Cu, Ni, Co, all
530 trivalent and tetravalent hydrolysates as shown in **Fig. 2**). This can be explained as preferential
531 retention of mineral components in thawing soils in the zone, and consequently, enhanced
532 mobilization of particulate organic carbon rather than silicate minerals from soil to river. The
533 later was demonstrated in a recent study of particulate nutrients across the WSL river gradient by

Krickov et al. (2018). This is also consistent with a local minimum of Si concentration in suspended matter of rivers having 20 to 30% of permafrost in their watersheds (**Fig. Supplement A**). The reason for the organic C maximum in the isolated to sporadic permafrost zone is that, at onset of permafrost appearance, soil water drains through the full depth of the unfrozen peat column which as a result provides mainly organic particles to the RSM.

In the northern, discontinuous and continuous permafrost zones, water travel time is much faster (Ala-aho et al., 2018) and runoff is higher (Nikitin and Zemtsov, 1986). Consequently, even small rivers exhibit a higher capacity for removal mineral sediments from soil horizons and, via bank abrasion, from former alluvial sediments within extended riparian zones. In this regard, the slower water flow in permafrost-free southern rivers is partially compensated by higher depth of active soil layer and possibility to mobilize mineral components by surface and shallow subsurface inflow to the river. As a result, both minimal capacity of surrounding soils to supply the mineral components to the river and the minimal ability of the river to mobilize mineral particles from riparian zone are encountered in rather narrow belt at the 'permafrost thaw front', in the isolated to sporadic zone.

4.3. Relative fraction of suspended over total (dissolved+suspened) elements in RSM of WSL

In permafrost-free watersheds, export of solid particles from the soil to the river occurs via lateral flow through the soil, oversurface flow in the forest floor, and by shallow groundwater discharge within the riparian or hyporheic zone. In the permafrost-affected territories, this transport is essentially controlled by suprapermafrost flow over the frozen layer via organic or mineral horizons. Although the mineral particles dominate the suspended load of all rivers regardless of size, the very small ones ($S_{watershed}$ < 100 km²) are strongly influenced by plant litter and organic detritus (Krickov et al., 2018). Irregular spatial and temporal delivery of these C-rich particles from soil to river produces much higher scattering in the particulate fraction value. Note

here that for soluble highly mobile elements such as B, Na, Ca, Sr the effect is less pronounced in large rivers compared to small ones: large rivers are subjected more to effects of deep groundwaters feeding through taliks. These underground waters are rich in dissolved (< 0.45 μm) soluble elements and poor in suspended matter. Because the role of underground feeding strongly decreases in permafrost-bearing rivers (Frey et al., 2007b; Pokrovsky et al., 2015), these elements exhibited an increase in particulate form with both latitude and permafrost coverage (see **Fig. S1 B, C**). This feature can be interpreted as due to diminishing of the effect of groundwater (dissolved form input) and the appearance of minerals (clay horizons) due to maximal deepening of the active layer. There was a decrease in the particulate fraction of Mg, Ca, Sr in large rivers compared to smaller ones (see example for Ca and Sr in **Fig. S1 A** and **D**, respectively). The most likely reason for this is enhanced feeding of large rivers through deep underground water located within calcareous collectors, as evidenced from dissolved (< 0.45 μm) element patterns across the WSL riverine transect (Pokrovsky et al., 2015, 2016).

In contrast, there was an increase in particulate versus total (particulate dissolved) transport of Al, Ga, Cr, Co, Mn, Fe, REE, and Ti, Zr, Hf, Th with an increase in watershed area (**Fig. 5 A, C, D**). Such a pattern can be explained by efficient mobilization to the river, via abrasion of river banks, of fine clays containing these low solubile immobile elements. Al exhibited strong increase in particulate fraction northward and with an increase in $S_{watershed}$ during all seasons (**Fig. 5 A**). Enhanced mobilization of particulate Al in northern rivers in autumn, at the maximum of active layer thickness, may be due to involvement of mineral horizon to soil water paths occurring at the end of summer season. An additional reason for the low particulate fraction of Al in small rivers draining peatlands is enrichment of these rivers in dissolved (< 0.45 μm) Al due to high DOC and low pH. As a result, the ratio of particulate Al to total Al in these small streams is lower than that in large rivers.

Among divalent heavy metals, only Mn, Ni and Cu demonstrated certain correlations of particulate fraction with landscape and permafrost parameters. The trend of increasing the

particulate transport of Mn with $S_{watershed}$ increase (**Fig. S2 D**) is interpreted as due to an increase in residence time of this element in rivers. This would lead to transformation of dissolved Mn^{2+}(aq) into particulate forms of $Mn^{(III, IV)}$ hydroxides via biotic and photochemical processes. Such processes were identified during the diurnal cycle of this element in boreal humic lakes (Pokrovsky and Shirokova, 2013) and also in boreal high latitude rivers (Ponter et al., 1992). Similarly, Ni and Cu exhibited an increase in suspended fraction with a decrease in watershed size (**Fig. S3 E**), especially visible in autumn for Cu ($R^2 = 0.32$, $p < 0.05$). This can be linked to Cu and Ni coprecipitation with/ adsorption onto Mn oxy(hydr)oxides. Additional point to consider is that this effect was consistent withan increase in C_{org} (RSM) in small rivers (Krickov et al., 2018) thereby demonstrating a close link between C and Cu. In autumn, there was an increase in particulate Cu share northward (**Fig. S3 F**) as well as an increase in lake and bog coverage of the watershed (**Fig. S3 C**). It could be linked to the coagulation of Cu-organic associates in lenthic waters and their release into the river system during autumn floods rain.

A specific feature of WSL rivers is impoverishment of their RSM relative to world average suspended load values in a number of low-solublity low-mobility elements such as certain divalent heavy metals, all trivalent hydrolysates and all tetravalent hydrolysates **(Fig. 6**). Typically, these elements are transported in essentially the particulate fraction but this is not the case for WSL rivers which demonstrate a high colloidal load (Pokrovsky et al., 2016b). For example, the proportion of suspended over total Fe in WSL rivers ranges from 95 to 30% (**Fig. S2**) whereas the majority of world rivers exhibit values between 99 and 80%; furthermore, the share of particulate Fe decreases down to 40% only in some organic-rich rivers (Olivié –Lauquet et al., 1999). Our results corroborate the former observations that, depending on the size of the river and organic matter content, Fe may occur as Fe-OM colloidal associates and iron hydroxide particles (Olivié –Lauquet et al., 2000). In WSL streams and rivers there is a continuum of colloidal and particulate Fe that is stabilized by organic matter (Pokrovsky et al., 2016b). We hypothesize that these organic and organo-mineral colloids are responsible for the sizeable

612 decrease in RSM fraction of low-soluble elements with $S_{watershed}$ decrease. Overall, compared to
613 the world average, WSL rivers exhibit relatively low amounts of suspended elements relative to
614 the total (suspended+dissolved) load due to 3 factors: 1) low runoff and low RSM concentration
615 as as a result of no bare rocks and mineral substrates exposed to physical weathering, 2) the
616 organic rather than mineral nature of surrounding "solid" substrates and the resulting high share
617 of organic matter in the RSM and 3) high DOC and Fe concentrations leading to a high
618 concentration of typically low-soluble elements in the dissolved (< 0.45 μm) fraction due to
619 colloids. In reference to the 2nd factor it is important to note that in spring, when the highest
620 RSM flux occurs, mineral soil horizons are fully frozen (Raudina et al., 2017).
621
622 *4.4. Mechanisms of RSM enrichment and impoverishment in elements and prospectives*
623 *for the permafrost thaw and climate change*
624 A cartoon of possible processes generating the suspended load on WSL rivers and the
625 RSM composition evolution under climate change and permafrost thaw is shown in **Fig. 8**. The
626 enrichment of river water in mineral and organic suspended particles occurs at the main channel
627 (via bank abrasion and resuspension of sediments at the floodplain) and in the thermokarst lakes
628 connected to rivers. Mobilization of particles rich in lithogenic elements from deep mineral
629 horizons and riparian sediments may occur via both bank erosion by flood and storm events and
630 through suprapermafrost flow in summer and autumn. The latter process is enhanced in the
631 presence of forests as trees increase the active layer thickness and allow soil fluids to reach the
632 mineral horizon and export particles via lateral flow to the river.
633 Within the climate change context in WSL, there are four main processes capable of
634 affecting RSM chemical composition as illustrated in **Fig. 8**: 1) a permafrost boundary shift
635 northward, consisting in disappearance of continuous permafrost in the north and replacement of
636 discontinuous permafrost by sporadic and isolated permafrost; 2) an increase in the ALT leading
637 to involvement of a deeper soil/rock horizon in vertical and lateral water movement in the south

638 which would extend the duration of period when soil pore fluids can enter and come into contact
639 with mineral layers under the peat horizon in the north; 3) a change of landscape environment
640 such as northward migration of the forest line, colonization of bogs by forest and dwarf shrubs
641 and thermokarst lake drainage; and 4) in the permafrost-affected part of WSL, the feeding of
642 rivers by underground water through taliks can raise the winter discharge of the rivers. Although
643 the 4th mechanism should not affect RSM chemical composition (except for Fe(III)
644 oxy(hydr)oxide formation due to Fe^{2+} oxidation), it does influence the dissolved (< 0.45 μm)
645 fraction of the river load (see discussion in Pokrovsky et al., 2015) and thereby controls the
646 change in suspended fraction over total (dissolved+suspended) transport.

647 Results obtained here allow first-order foresight on the effect of climate warming and
648 permafrost thaw on major and trace element concentrations in the suspended load of WSL rivers.
649 The concept of "substituting space for time" in the WSL (Frey et al., 2007 a, b; Frey and Smith,
650 2005) implies a shift of the permafrost boundary to northward combined with simultaneous increase
651 in ALT (**Fig. 8**). On a short-term scale (10 to 100 years) this may reconfigure permafrost
652 distribution as following: continuous → discontinuous; discontinuous → sporadic; sporadic →
653 isolated, isolated → absent. The U-shape dependences of most element concentration on
654 permafrost type demonstrate a minimum at the beginning of permafrost thaw, in sporadic to
655 discontinuous permafrost zones (**Fig. 2**). This concentration pattern implies that, upon a
656 progressive shift of the permafrost boundary northward, there will be sizeable decrease in the
657 concentration of alkalis, alkaline-earths, divalent heavy metals, and trivalent and tetravalent
658 hydrolysates in northern rivers in currently discontinuous and continuous permafrost zones. This
659 decrease may be a factor of 2 to 5 as follows from the position of the minimum elemental
660 concentration in sporadic to discontinuous permafrost zones relative to the continuous
661 permafrost zone (**Fig. 2**).

662 Moreover, an increase in the ALT will likely increase the particulate fraction in total
663 element transport for many soluble (labile) and also lithogenic elements in WSL rivers, as more

mineral horizons (currently frozen under the peat layer) will be involved in water drainage and lateral export through soils. Specifically, if the current rate of soil warming persists, the active layer thickness may reach 4 m in the tundra of Yamal Peninsula, which is currently continuous permafrost zone, by the year 2100 (Sudakov et al., 2011). These changes will certainly produce much deeper water paths toward mineral soils and underlying sand, silt and clay deposits. As a result, the concentration of particulate lithogenic elements in the northern part of WSL may increase. On a long-term scale (100 to 1000 years), forests will progressively take over bogs and lakes and the permafrost-bearing territory will become a permafrost-free one. Regardless of season, an increase in forest proportion within the river watershed will inevitably increase concentrations of many elements (all alkalis and alkaline-earths, B, Mn, Co, As, Al, Ga, REEs, Nb, Ti, Zr, Hf, Th) in the permafrost-bearing zone. Although this increase is unlikely to offset the predicted decrease in concentration due to permafrost boundary shift northward, the overall impact of permafrost thaw and vegetation rise on element concentrations in RSM may be more complex than what follows from a mere shift in the permafrost boundary northward.

As for the evolution of particulate element fraction over total (dissolved + particulate) form, the increase in water connectivity between deep underground reservoirs and rivers due to permafrost thaw and the widespread appearance of taliks may increase the input of dissolved elements thereby further decreasing the already low share of particulate forms to total element export from the WSL territory to the Arctic Ocean. In this regard, peatlands of continental planes having low runoff may represent an exception compared to rivers of other mountainous subarctic regions. The latter will certainly increase their particulate flux following gradual increase in precipitation and ALT as well as abrupt permafrost thaw.

CONCLUSIONS

In order to resolve poorly known features of chemical composition of river suspended particles in the permafrost region, we measured major and trace elements in RSM of 33 western

690 Siberian rivers during different seasons. The concentration of all elements in the RSM followed
691 the order "spring > summer ≥ autumn". This order reflects the capacity of running water to
692 mobilize relatively heavy (compared to peat) mineral particles via bank abrasion, resuspension in
693 riparian zone, and lateral influx from soils via shallow subsurface and suprapermafrost flow.

694 The forest acted as an important source of elements in RSM as it enhanced the water path
695 down to mineral horizons leading to physical erosion, breakdown of soil mineral particles via
696 biological activity in the deep rooting zone thereby facilitating delivery of particles from deep
697 soil horizons to susbsurface inflow to the river. The lakes and bogs mainly retained mineral
698 particles while generating C-rich RSM; however this was observed only for permafrost-bearing
699 zone. The RSM enrichment in the soluble highly mobile elements (alkalis, alkaline earths)
700 fraction for northern rivers is due to lower transport of the dissolved (< 0.45 μm) fraction for
701 these elements in permafrost-bearing zones, where, compared to southern rivers, the
702 underground feeding of rivers from carbonate-hosted deep rocks is not pronounced.

703 Compared to the other rivers of the world, the WSL rivers exhibited low suspended
704 fraction of insoluble trace elements, presumably due to colloidal transport provided by high
705 DOC and Fe concentration. We observed minimal concentrations of trace element in the RSM of
706 isolated and sporadic permafrost zone. Using a "substituting space for time' concept for
707 predicting future changesin river chemistry, we foresee that the permafrost boundary shift may
708 sizeably (2 to 5 times) decrease major and TE concentrations in RSM of northern rivers located
709 in discontinuous to continuous permafrost zones; the forest line migration northward may only
710 partially offset this decrease. At the same time, the increase in active layer thickness may enrich
711 the RSM in lithogenic low soluble elements.

712

713 **Acknowledgements:**
714 We acknowledge the main support from an RSCF (RNF) grant No 18-17-00237 "Mechanisms of
715 hydrochemical runoff of the Ob River…" and partial funding from RFFI (RFBR) grants No 16-

716 34-60203-mol_a_dk, 18-35-00563\18, and 19-55-15002. Chris Benker is thanked for English
717 proofread corrections.

718

719 **References**

720 Ala-Aho P., Soulsby C., Pokrovsky O.S., Kirpotin S.N., Karlsson J., et al. (2018) Using stable
721 isotopes to assess surface water source dynamics and hydrological connectivity in a high-
722 latitude wetland and permafrost influenced landscape. *J. Hydrol.,* **556,** 279–293.
723 Andersson P.S., Porcelli D., Wasserburg G.J., Ingri J. (1998) Particle transport of ^{234}U-^{238}U in
724 the Kalix River and in the Baltic Sea. *Geochim. Cosmochim. Acta* **62**(3), 385-392.
725 Baturin G.N. and Gordeev V.V. (2019) Geochemistry of suspended matter in the Amazon River
726 waters. *Geochemistry Internat.,* **57**(2), 197–205.
727 Blois J.L., Williams J.W., Fitzpatrick M.C., Jackson S.T., Ferrier S. (2013) Space can substitute
728 for time in predicting climate-change effects on biodiversity. *PNAS,* **110**(23), 9374-9379.
729 Bring A., Fedorova I., Dibike Y., Hinzman L., Mard J., Mernild S.H., Prowse T., Semenova O.,
730 Stuefer S.L., Woo M.-K. (2016) Arctic terrestrial hydrology: A synthesis of processes,
731 regional effects, and research challenges. *J. Geophys Res: Biogeosci.*, **121**(3), 621–649.
732 Cooper L.W., McClelland J.W., Holmes R.M., Raymond P.A., Gibson J.J., Guay C.K., Peterson
733 B.J. (2008). Flow-weighted values of runoff tracers ($\delta^{18}O$, DOC, Ba, alkalinity) from the six
734 largest Arctic rivers. *Geophys. Res. Lett.*, **35**(18), https://doi.org/10.1029/2008gl035007.
735 Drake T.W., Tank S.E., Zhulidov A.V., Holmes R.M., Gurtovaya T., Spencer R.G.M. (2018)
736 Increasing alkalinity export from large Russian Arctic River. *Environ. Sci. Technol.*, **52**(15),
737 8302-8308.
738 Frappart F., Papa F., Güntner A., Susanna W., Ramillien G., Prigent C., Rossow W.B., Bonnet
739 M.P. (2010). Interannual variations of the terrestrial water storage in the Lower Ob' Basin
740 from a multisatellite approach. *Hydrol. Earth Syst. Sc.*, **14**(12), 2443-2453.
741 Frey K.E., McClelland J.W., Holmes R.M., Smith L.C. (2007a) Impacts of climate warming and
742 permafrost thaw on the riverine transport of nitrogen and phosphorus to the Kara Sea. *J.*
743 *Geophys. Res: Biogeosciences,* **112**(G4), https://doi.org/10.1029/2006JG000369.
744 Frey K.E., Siegel D.I., Smith L.C. (2007b) Geochemistry of west Siberian streams and their
745 potential response to permafrost degradation. *Water Resour. Res.*, **43**(3),
746 https://doi.org/10.1029/2006WR004902
747 Frey K.E., Smith L.C. (2005) Amplified carbon release from vast West Siberian peatlands by 2100.
748 *Geophys. Res. Lett*., **32**(9), https://doi.org/10.1029/2004GL022025
749 Frey K.E. and McClelland J.W. (2009) Impacts of permafrost degradation on arctic river
750 biogeochemistry. *Hydrol. Process.*, **23**(1), 169–182.
751 Gaillardet J., Millot R., Dupré B. (2003) Chemical denudation rates of the western Canadian
752 orogenic belt: the Stikine terrane. *Chem. Geol.,* **201**(3-4), 257-279.
753 Gebhardt A.C., Gaye-Haake B., Unger D., Lahajnar N., Ittekkot V. (2004) Recent particulate
754 organic carbon and total suspended matter fluxes from the Ob and Yenisei Rivers into the
755 Kara Sea (Siberia). *Mar. Geol.*, **207**(1-4), 225–245.
756 Gislason S.R., Oelkers E.H., Snorrason A. (2006) Role of river-suspended material in the global
757 carbon cycle. *Geology*, **34**(1), 49-52.
758 Goncharova O.Y., Matyshak G.V., Bobrik A.A., Moskalenko N. G., Ponomareva O. E. (2015)
759 Temperature regimes of northern taiga soils in the isolated permafrost zone of Western
760 Siberia. *Eurasian Soil Sci*., **48**(12), 1329–1340.
761 Goncharova O.Y., Bobrik A.A., Matyshak G.V., Makarov M.I. (2016) The role of soil cover in
762 maintaining the structural and functional integrity of northern taiga ecosystems in Western
763 Siberia. *Contemp. Probl. Ecol*., **9**(1), 1–8.

764 Gordeev V.V. (2000) River input of water, sediment, major elements, nutrients and trace metals
765 from Russian territory to the Arctic ocean. In: *The Freshwater Budget of the Arctic Ocean*,
766 E.L.Lewis-ed., Dordrecht et al.: Kluwer, p. 297-322.
767 Gordeev, V.V., Lisitzin A.P. (2014) Geochemical interaction between the freshwater and marine
768 hydrospheres. *Russ. Geol. Geophys*., **55**, 561-581.
769 Gordeev V.V., Rachold V., Vlasova I.E. (2004) Geochemical behaviour of major and trace
770 elements in suspended particulate material of the Irtysh river, the main tributary of the Ob
771 river, Siberia. *Appl. Geochem*., **19**(4), 593-610. doi: 10.1016/j.apgeochem.2003.08.004
772 Gordeev V.V., Martin J.M., Sidorov I.S., Sidorova M.V. (1996) A reassessment of the Eurasian
773 river input of water, sediment, major elements, and nutrients to the Arctic Ocean. *Am. J. Sci.*,
774 **296**(6), 664–691.
775 Guo L., Zhang J. Z., Guéguen C. (2004) Speciation and fluxes of nutrients (N, P, Si) from the upper
776 Yukon River. *Global Biogeochem. Cy.*, **18**(1), https://doi.org/10.1029/2003GB002152
777 Gurvich E.G., Isaeva A.B., Dyomina L.V., Levitan M.A., Muravyov K.G. (1995) Chemical
778 composition of bottom sediments from the Kara Sea and estuaries of the Ob and Yenisey
779 Rivers. *Oceanology,* **34**(5), 701-709.
780 Heinze C., Meyer S., Goris N., Anderson L., Chang N., Le Quéré C., Bakker D.C.E. (2015) The
781 ocean carbon sink – impacts, vulnerabilities and challenges. *Earth Syst. Dynam*., **6**, 327–358.
782 Hobbie J.E., Peterson B.J., Bettez N. Deegan L., O'Brien W.J, Kling G.W., Kipphut G.W., Bowden
783 W.B., Hershey A.E. (1999) Impact of global change on the biogeochemistry and ecology of an
784 Arctic freshwater system. *Polar Res*., **18**(2), 207– 214.
785 Holmes R.M., Peterson B. J., Gordeev V.V., Zhulidov A.V., Meybeck M., Lammers R.B.,
786 Vorosmarty C.J. (2000) Flux of nutrients from Russian rivers to the Arctic Ocean: Can we
787 establish a baseline against which to judge future changes? *Water Resour. Res*., **36**(8), 2309–
788 2320.
789 Holmes R. M., Peterson B. J., Zhulidov A.V., Gordeev V. V., Makkaveev P. N., Stunzhas P. A.,
790 Kosmenko L.S., Kohler G.H., Shiklomanov A.I. (2001) Nutrient chemistry of the Ob' and
791 Yenisey Rivers, Siberia: results from June 2000 expedition and evaluation of long-term data
792 sets. *Mar. Chem*., **75**(3), 219–227.
793 Holmes R.M., McClelland J.W., Peterson B.J., Tank S.E., Bulygina E., Eglinton T.I., Gordeev
794 V.V., Gurtovaya T.Y., Raymond P.A., Repeta D.J., Staples R., Striegl R.G., Zhulidov A.V.,
795 Zimov S.A. (2012) Seasonal and annual fluxes of nutrients and organic matter from large rivers
796 to the Arctic Ocean and surrounding seas. *Estuaries Coasts,* **35**(2), 369–382.
797 Holmes R.M., McClelland J.W., Peterson B.J., Shiklomanov I.A., Shiklomanov A.I., Zhulidov
798 A.V., Gordeev V.V., Bobrovitskaya N.N. (2002) A circumpolar perspective on fluvial
799 sediment flux to the Arctic ocean. *Global Biogeochem. Cy.*, **16**(4), 45-1-45–14.
800 https://doi.org/10.1029/2001gb001849
801 Javed M.B., Shotyk W. (2018) Estimatin bioaccessibility of trace elements in particles suspended
802 in the Athabasca River using sequential extraction. *Environ. Pollut.*, 240, 466-474.
803 Kaiser K., Canedo-Oropeza M., McMahon R., Amon R.M.W. (2017). Origins and transformations
804 of dissolved organic matter in large Arctic rivers. *Sci. Reports*, **7**(1), 13064.
805 Khrenov V.Y. (2011) Soils of cryolithozone of western Siberia: Morphology, physico-chemical
806 properties and geochemistry. *Nauka, Novosibirsk*. pp. 211 (in Russian).
807 Kremenetski K.V., Velichko A.A., Borisova O.K., MacDonald G.M., Smith L.C., Frey K.E.,
808 Orlova L.A. (2003) Peatlands of the West Siberian Lowlands: Current knowledge on
809 zonation, carbon content, and Late Quaternary history. *Quaternary Sci. Rev.,* **22**(5-7), 703–
810 723.
811 Krickov I., Lim A., Manasypov R.M., Loiko S.V., Shirokova L.S., Kirpotin S.N., Karlsson J.,
812 Pokrovsky O.S. (2018) Riverine particulate C and N generated at the permafrost thaw front:
813 case study of western Siberian rivers across a 1700-km latitudinal transect. *Biogeosciences*
814 **15,** 6867–6884, https://doi.org/10.5194/bg-15-6867-20.

Kutscher L., Mörth C.-M., Porcelli D., Hirst C., Maximov T. C., Petrov R. E., and Andersson P. S. (2017) Spatial variation in concentration and sources of organic carbon in the Lena River, Siberia. *J. Geophys. Res.-Biogeo.*, **122**(8), 1999–2016.

Kulizhskiy S.P., Loyko S.V., Gerber A.A. (2017a) Distribution patterns of soils in the forest tundra of West Siberia (right bank in the middle of the river Pur). *Vestnik Orenburg State University*, **211**(11), 93–97 (in Russian).

Kulizhskii S.P., Loiko S.V., Morgalev Yu.N., Istigechev G.I., Rodikova A.V., Maron T.A. (2017b) Investigation of platinum and nickel nanoparticles migration and accumulation in soils within the Southeastern part of West Siberia. *Nano Hybrids Composites* **13,** 115–122. doi:10.4028/www.scientific.net/NHC.13.115

Lim A.G., Loiko S.V., Kritckov I.V., Kyzmina D.M. (2017) Structural-functional features of landscapes with active thermocarst in the northern taiga of Western Siberia. *Ukrainian J. Ecology*, **7**(4), 414–423.

Lisitzin A.P., Lukashin V.N., and Dara O.M. (2015) Composition and fluxes of minerals in suspended particulate matter from the water column of the Caspian Sea. *Dokl. Earth Sci.,* **463,** 733–737, https://doi.org/10.1134/S1028334X15070120.

Lobbes J. M., Fitznar H. P., and Kattner G. (2000) Biogeochemical characteristics of dissolved and particulate organic matter in Russian rivers entering the Arctic Ocean. *Geochim. Cosmochim. Ac*., **64**(17), 2973–2983.

Loiko S.V., Pokrovsky O.S., Raudina T., Lim A., Kolesnichenko L.G., Shirokova L.S., Vorobyev S.N., Kirpotin S.N. (2017) Abrupt permafrost collapse enhances organic carbon, CO_2, nutrient, and metal release into surface waters. *Chem.Geol*., **471**, 153–165.

Loiko S.V., Geras'ko L.I., Kulizhskii S.P., Amelin I.I., Istigechev G.I. (2015) Soil cover patterns in the northern part of the area of aspen-fir taiga in the southeast of Western Siberia. *Eurasian Soil Science* **48** (4), 359–372, doi: 10.1134/S1064229315040067.

Loiko S.V., Pokrovsky O.S., Raudina T.V., Lim A., Kolesnichenko L.G., Shirokova L.S., Vorobyev S.N., Kirpotin S.N. (2017). Abrupt permafrost collapse enhances organic carbon, CO_2, nutrient and metal release into surface waters. *Chem. Geol.*, **471**, 153–165.

Magritsky D.V. (2010) Annual suspended matter flow of the Russian rivers belonging to the Arctic Ocean basin and its anthropogenic transformation. *Vestn. Mosk. Univ. Ser. Geogr.*, **5**, 17-24. (in Russian)

McClelland J.W., Townsend-Small A., Holmes R. M., Pan F., Stieglitz M., Khosh M., Peterson B. J. (2014) River export of nutrients and organic matter from the North Slope of Alaska to the Beaufort Sea. *Water Resour. Res*., **50**(2), 1823-1839.

McClelland J.W., Holmes R.M., Raymond P.A., Striegl R.G., Zhulidov A.V., Zimov S.A., Zimov N., Tank S.E., Spencer R.G.M., Staples R., Gurtovaya T.Y., Grif C.G. (2016). Particulate organic carbon and nitrogen export from major Arctic rivers. *Global Biogeochem. Cy.*, **30**(5), 629-643.

Meybeck M. (1982). Carbon, nitrogen, and phosphorus transport by world rivers. *Am. J. Sci.,* **282**(4), 401-450.

Millot R., Vigier N., Gaillardet J. (2010) Behaviour of lithium and its isotopes during weathering in the Mackenzie Basin, Canada. *Geochim. Cosmochim. Acta,* **74**(14), 3897-3912.

Morozov N.P., Baturin G.N., Gordeev V.V., Gurvich E.G. (1974) On the composition of suspended and bottom sediments in the mouth areas of the Severnaya Dvina, Mezen, Pechora and Ob'. *Hydrochemical Materials*, **60**, 60-73.

Nikanorov A.M., Smirnov M.P., Klimenko O.A. (2010) Long-term trends in total and anthropogenic discharge of organic and biogenic substances by Russian rivers into the Arctic and Pacific Seas. *Water Res*., **37**(3), 361-371.

Nikitin S. P. and Zemtsov V. A.(1986) The variability of hydrological parameters of western Siberia, Nauka, Novosibirsk. pp. 204.

O'Donnell J.A., Aiken G.R., Swanson D.K., Panda S., Butler K.D., Baltensperger A.P. (2016) Dissolved organic matter composition of Arctic rivers: Linking permafrost and parent material to riverine carbon, *Global Biogeochem. Cy.*, **30**(1), 1811–1826.

Olivié-Lauquet G., Allard T., Benedetti M., Muller J.P. (1999) Chemical distribution of trivalent iron in riverine material from a tropical ecosystem: A quantitative EPR study. *Water Res.*, **33**(11), 2726-2734.

Olivié-Lauquet G., Allad T., Bertaux J., Muller J.P. (2000) Crystal chemistry of suspended matter in a tropical hydroxystem, Nyong basin (Cameroon, Africa). *Chem. Geol.,* **170**(1-4), 113-131.

Pokrovsky O.S., Schott J., Kudryavtsev D.I., Dupré B. (2005) Basalts weathering in Central Siberia under permafrost conditions. *Geochim. Cosmochim. Ac.*, **69**(24), 5659-5680.

Pokrovsky O.S., Schott J., Dupré B. (2006) Trace elements fractionation and transport in boreal streams and soil solutions of basaltic terrain, Central Siberia. *Geochim. Cosmochim. Ac.*, **70**, 3239-3260.

Pokrovsky O.S., Viers J., Shirokova L.S., Shevchenko V.P., Filipov A.S., Dupré B. (2010) Dissolved, suspended, and colloidal fluxes of organic carbon, major and trace elements in Severnaya Dvina River and its tributary. *Chem. Geol.*, **273**(1-2), 136–149.

Pokrovsky O.S., Shirokova L.S. (2013) Diurnal variations of dissolved and colloidal organic carbon and trace metals in a boreal lake during summer bloom. *Water Res.*, **47**(2), 922–932.

Pokrovsky O.S., Manasypov R.M., Shirokova L.S., Loiko S.V., Krickov I.V., Kopysov S. et al., (2015) Permafrost coverage, watershed area and season control of dissolved carbon and major elements in western Siberia rivers. *Biogeosciences*, **12**, 6301–6320.

Pokrovsky O.S., Manasypov R.M., Loiko S., Krickov I.A., Kopysov S.G., Kolesnichenko L. G., Vorobyev S.N., Kirpotin S.N. (2016a) Trace element transport in western Siberia rivers across a permafrost gradient. *Biogeosciences*. **13**(6), 1877–1900.

Pokrovsky O.S., Manasypov R.M., Loiko S.V., Shirokova L.S., (2016b) Organic and organo-mineral colloids of discontinuous permafrost zone. *Geochim. Cosmochim. Ac.*, **188,** 1–20.

Polishchuk Y.M., Bogdanov A.N., Polischuk V.Y., Manasypov R.M., Shiorkova L.S., Kirpotin S.N., Pokrovsky O.S. (2017) Size-distribution, surface coverage, water, carbon and metal storage of thermokarst lakes (> 0.5 ha) in permafrost zone of the Western Siberia Lowland. *Water-Sui.,* **9**(3), 228. doi:10.3390/w9030228.

Polishchuk Y.M., Bogdanov A.N., Muratov I.N., Polishchuk V.Y., Lim A., Manasypov R.M., Shirokova L.S., Pokrovsky O.S. (2018) Minor contribution of small thaw ponds to the pools of carbon and methane in the inland waters of the permafrost-affected part of western Siberian Lowland. *Environ. Res. Lett.*, **13**(4), 045002. https://doi.org/10.1088/1748-9326/aab046

Ponter C., Ingri J., Boström K. (1992) Geochemistry of manganese in the Kalix River, northern Sweden. *Geochim. Cosmochim. Ac.,* **56**, 1485-1494.

Quénard L., Samouëlian A., Laroche B., Cornu S. (2011) Lessivage as a major process of soil formation: a revisitation of existing data. *Geoderma,* **167–168,** 135–147.

Raudina T.V, Loiko S.V., Lim A.G., Krickov I.V., Shirokova L.S., Istignichev G.I., Kuzmina D.M., Kulizhsky S.P., Vorobyev S.N., Pokrovsky O.S. (2017) Dissolved organic carbon and major and trace elements in peat porewater of sporadic, discontinuous, and continuous permafrost zones of western Siberia. *Biogeosciences*, **14**(14), 3561–3584.

Raudina T.V., Loiko S.V., Lim A., Manasypov R.M., Shirokova L.S., Istigecgev G.I., Kuzmina D.M., Kulizhsky S.P., Vorobyev S.N., Pokrovsky O.S. (2018) Permafrost thaw and climate warming may decrease the CO_2, carbon, and metal concentration in peat soil waters of the Western Siberia Lowland. *Sci. Total Environ.*, **634**, 1004-1023.

Romanovsky V. E., Drozdov D. S., Oberman N. G., Malkova G. V., Kholodov A. L., et al., (2010) Thermal state of permafrost in Russia. *Permafrost Periglac.*, **21**(2), 136–155.

Sabrekov A. F., Runkle B. R. K., Glagolev M. V., Terentieva I. E., Stepanenko V. M., Kotsyurbenko O. R., Maksyutov S. S. and Pokrovsky O. S. (2017) Variability in methane emissions from West Siberia's shallow boreal lakes. *Biogeosciences,* **14**(15), 3715-3742.

Savenko V.S., Pokrovskii O.S., Dupré B., Baturin G.N. (2004). The chemical composition of suspended matter of major rivers of Russia and adjacent countries. *Dokl. Earth Sci.*, **398**(7), 938-942.

Savenko, V.S. (2006) Principal features of the chemical composition of suspended load in world rivers. *Dokl. Earth Sci.*, **407**(2), 450-454.

Schlesinger W. H., Melack J. M. (1981) Transport of organic carbon in the world's rivers. *Tellus*, **33**(2), 172–187. https://doi.org/10.3402/tellusa.v33i2.10706

Serikova S., Pokrovsky O.S., Ala-Aho P., Kazantsev V., Kirpotin S., et al. (2018) High riverine CO_2 emissions at the permafrost boundary of Western Siberia. *Nat. Geosci.*, **11,** 825-829, https://doi.org/10.1038/s41561-018-0218-1.

Serikova S., Pokrovsky O.S., Laudon H., Krickov I.V., Lim A.G., Manasypov R.M., Karlsson J. (2019) High carbon emissions from thermokarst lakes of Western Siberia. *Nature Comm.,* **10,** Art No 1552. https://doi.org/10.1038/s41467-019-09592-1.

Shevchenko V.P., Pokrovsky O.S., Filipov A.S., Lisitzin A.P., Bobrov V.A., Bogunov A.Y., Zavernina N.N., et al. (2010) On the elemental composition of suspended matter of the Severnaya Dvina river (White Sea region). *Dokl. Earth Sci.*, **430**(2), 228-234. doi: 10.1134/S1028334X10020182.

Shevchenko V.P., Pokrovsky O.S., Vorobyev S.N., Krickov I.V., Manasypov R.M., et al. (2017) Impact of snow deposition on major and trace element concentrations and fluxes in surface waters of Western Siberian Lowland. *Hydrol. Earth Syst.Sc.*, **21**(11), 5725–5746, https://doi.org/10.5194/hess-21-5725-2017.

Shirokova L. S., Pokrovsky O. S., Kirpotin S. N., Desmukh C., Pokrovsky B. G., Audry S. and Viers J. (2013) Biogeochemistry of organic carbon, CO_2, CH_4, and trace elements in thermokarst water bodies in discontinuous permafrost zones of Western Siberia. *Biogeochemistry,* **113**(1-3), 573–593.

Shirokova L.S., Labouret J., Gurge M., Gerard E., Zabelina S.A., Ivanova I.S., Pokrovsky O.S. (2017) Impact of cyanobacterial associate and heterotrophic bacteria on dissolved organic carbon and metal in moss and peat leachate: application to permafrost thaw in aquatic environments. *Aquat. Geochem.*, **23**(5–6), 331–358.

Stedmon C. A., Amon R. M. W., Rinehart A. J., Walker S. A. (2011) The supply and characteristics of colored dissolved organic matter (CDOM) in the Arctic Ocean: Pan Arctic trends and differences. *Mar. Chem.,* **124**(1-4), 108–118.

Stepanova V.M., Pokrovsky O.S., Viers J., Mironycheva-Tokareva N.P. Kosykh N.P., Vishnyakova E.K. (2015) Elemental composition of peat profiles in western Siberia: Effect of the micro-landscape, latitude position and permafrost coverage. *Appl. Geochem.*, **53**, 53–70.

Sudakov I.A., Bobylev L.P., Beresnev S.A. (2011) Modeling of thermal regime of permafrost during contemporary climate change. *Vestnik St Petersbourg University*, **7**(1), 81-88. (in Russian) http://vestnik.spbu.ru/pdf11/s07/s07v1_11.pdf.

Tank S.E., Frey K.E., Striegl R.G., Raymond P.A., Holmes R.M., McClelland J.W., Peterson B.J. (2012a) Landscape-level controls on dissolved carbon flux from diverse catchments of the circumboreal. *Global Biogeochem. Cy.*, **26**(4), https://doi.org/10.1029/2012GB004299.

Tank S.E., Manizza M., Holmes R.M., McClelland J.W., and Peterson B.J. (2012b) The processing and impact of dissolved riverine nitrogen in the Arctic Ocean. *Estuaries Coasts*, **35**(2), 401-415.

Tank S.E., Striegl R.G., McClelland J.W., Kokelj S.V. (2016) Multi-decadal increases in dissolved organic carbon and alkalinity flux from the Mackenzie drainage basin to the Arctic Ocean. *Environ. Res. Lett.*, **11**(5), 54015. https://doi.org/10.1088/1748-9326/11/5/054015

Tonkonogov V.D. (1999) Clay-differentiated soils of European Russia. Dokuchaev Soil Institute, Moscow (in Russian)

Toohey R.C., Herman-Mercer N.M., Schuster P.F., Mutter E.A., Koch J.C. (2016) Multi-decadal increases in the Yukon River Basin of chemical fluxes as indicators of changing flowpaths, groundwater, and permafrost. *Geophys. Res. Lett.,* **43**(23), https://doi.org/10.1002/2016GL070817

Viers J., Dupré B., Gaillardet J. (2009) Chemical composition of suspended sediments in World Rivers : New insights from a new database. *Sci. Total Environ.* **407**(2), 853-863.

Vonk J.E., Tank S.E., Bowden W.B., Laurion I., Vincent W.F., et al. (2015) Reviews and syntheses: Effects of permafrost thaw on Arctic aquatic ecosystems. *Biogeosciences*, **12**(23), 7129-7167.

Vorobyev S.N., Pokrovsky O.S., Serikova S., Manasypov R.M., Krickov I.V., Shirokova L.S., Lim A., Kolesnichenko L.G., Kirpotin S.N., Karlsson J. (2017) Permafrost boundary shift in western Siberia may not modify dissolved nutrient concentrations in rivers. *Water,* **9**(12), 985, doi:10.3390/w9120985.

Yeghicheyan D., Bossy C., Bouhnik Le Coz M., Douchet Ch., Granier G., Heimburger A., Lacan F., Lanzanova A., Rousseau T.C.C., Seidel J.-L., Tharaud M., Candaudap F., Chmeleff J., Cloquet C., Delpoux S., Labatut M., Losno R., Pradoux C., Sivry Y., and Sonke J.E. (2013) A Compilation of silicon, rare earth element and twenty-one other trace element concentrations in the natural river water reference material SLRS-5 (NRC-CNRC), *Geostand. Geoanal. Res.,* **37,** 449–467, doi:10.1111/j.1751-908X.2013.00232.x.

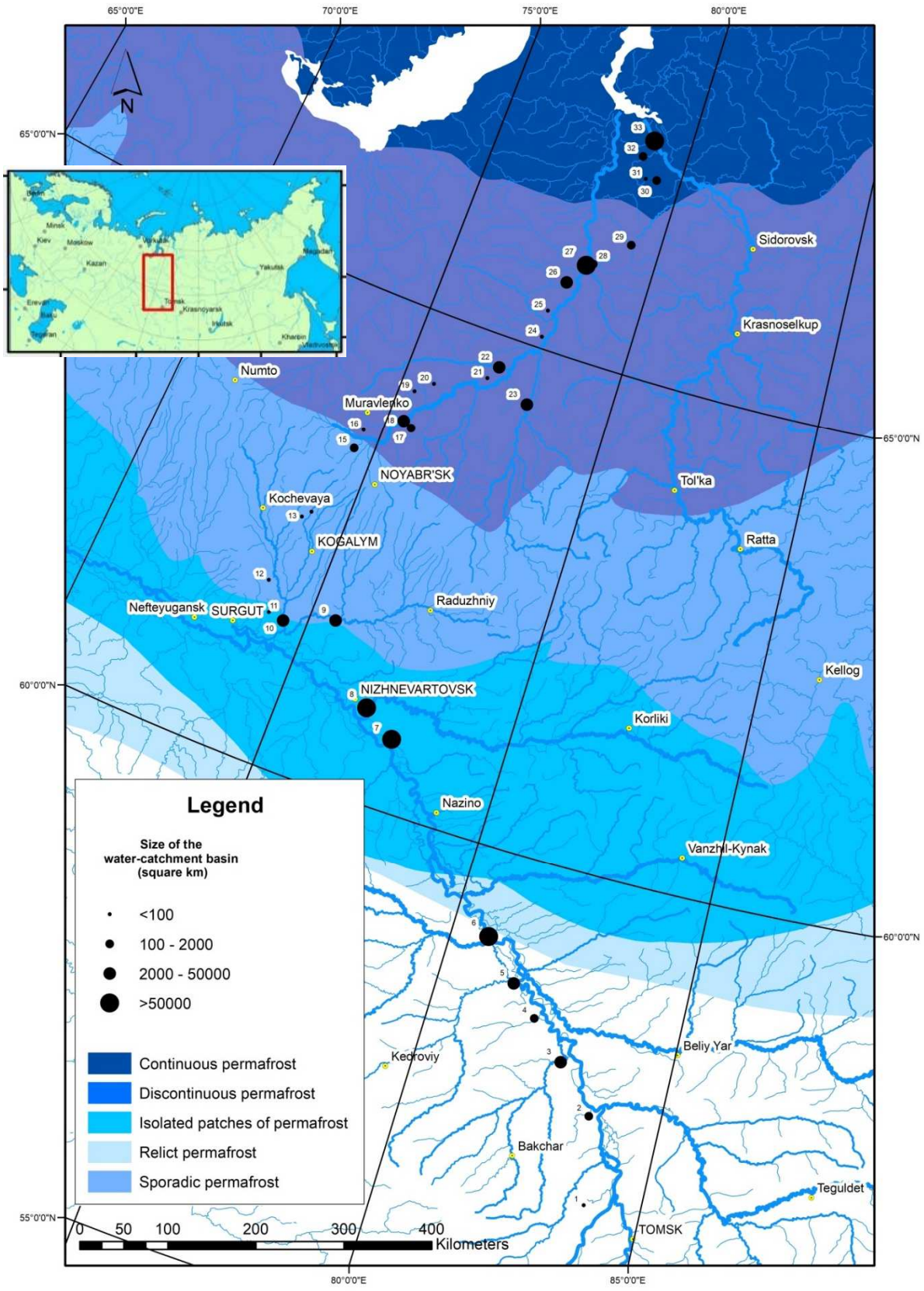

987

988 **Fig. 1.** Sampling sites and physio-geographical context of WSL territory investigated in this

989 work. The sampling numbers are explained in Table S1.

990

991

992 **1st group**

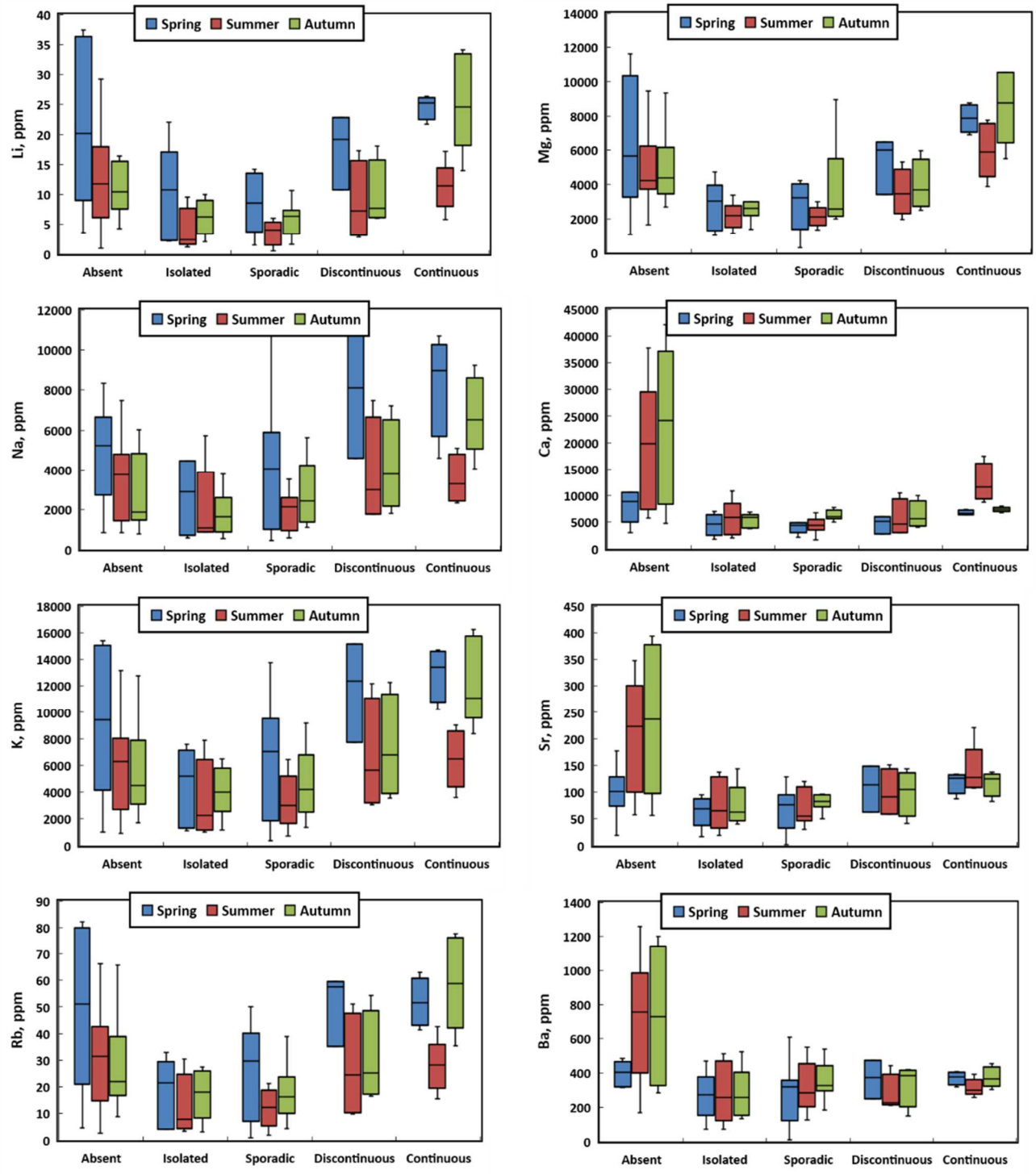

993

994

995

996

997 **Fig. 2.** Box plot of first and third quartiles (25 and 75%) of 5 groups of elements in the

998 suspended matter of WSL rivers.

999

1000 **2nd group**

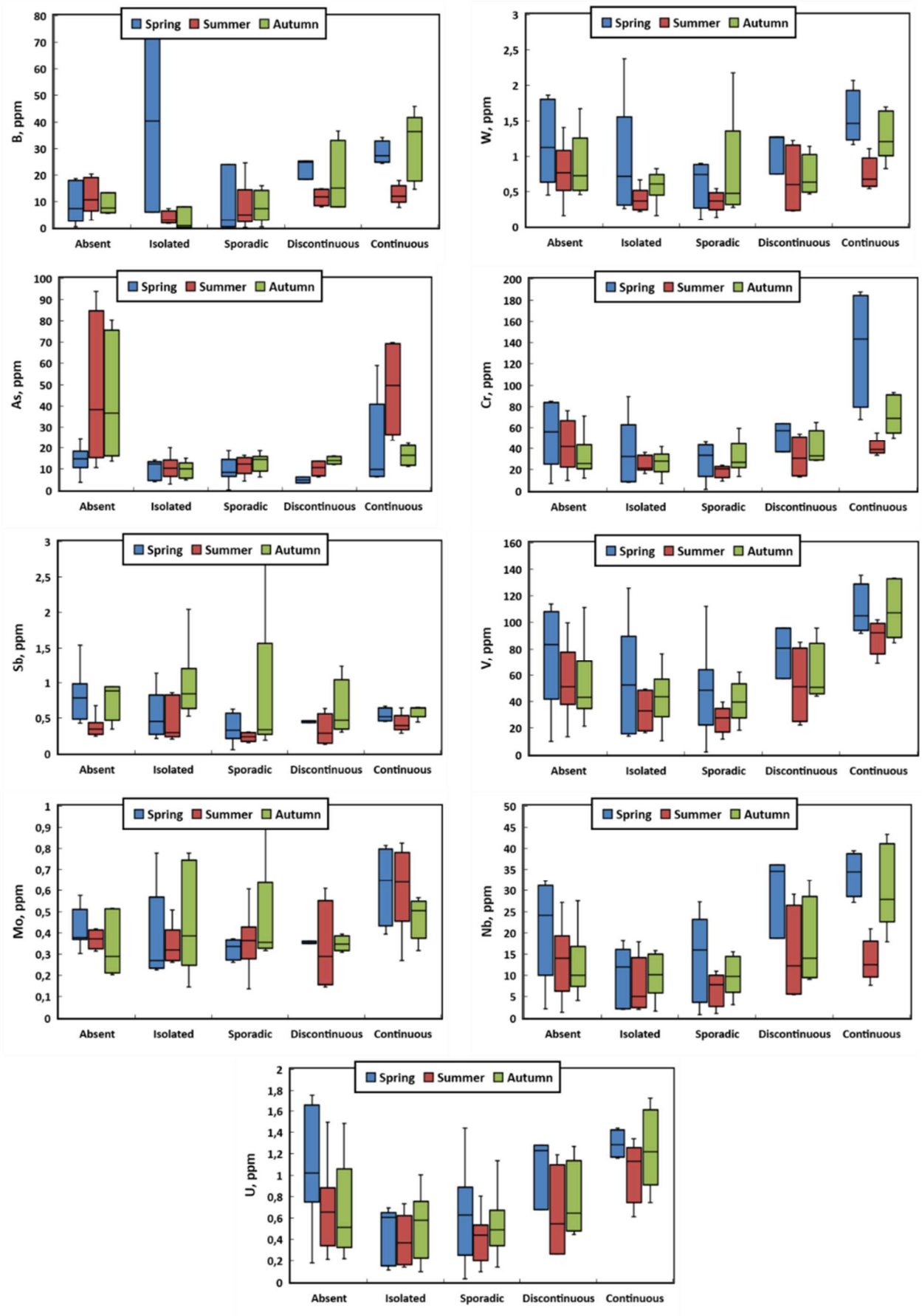

1001

1002 **Fig 2**, continued

3rd group

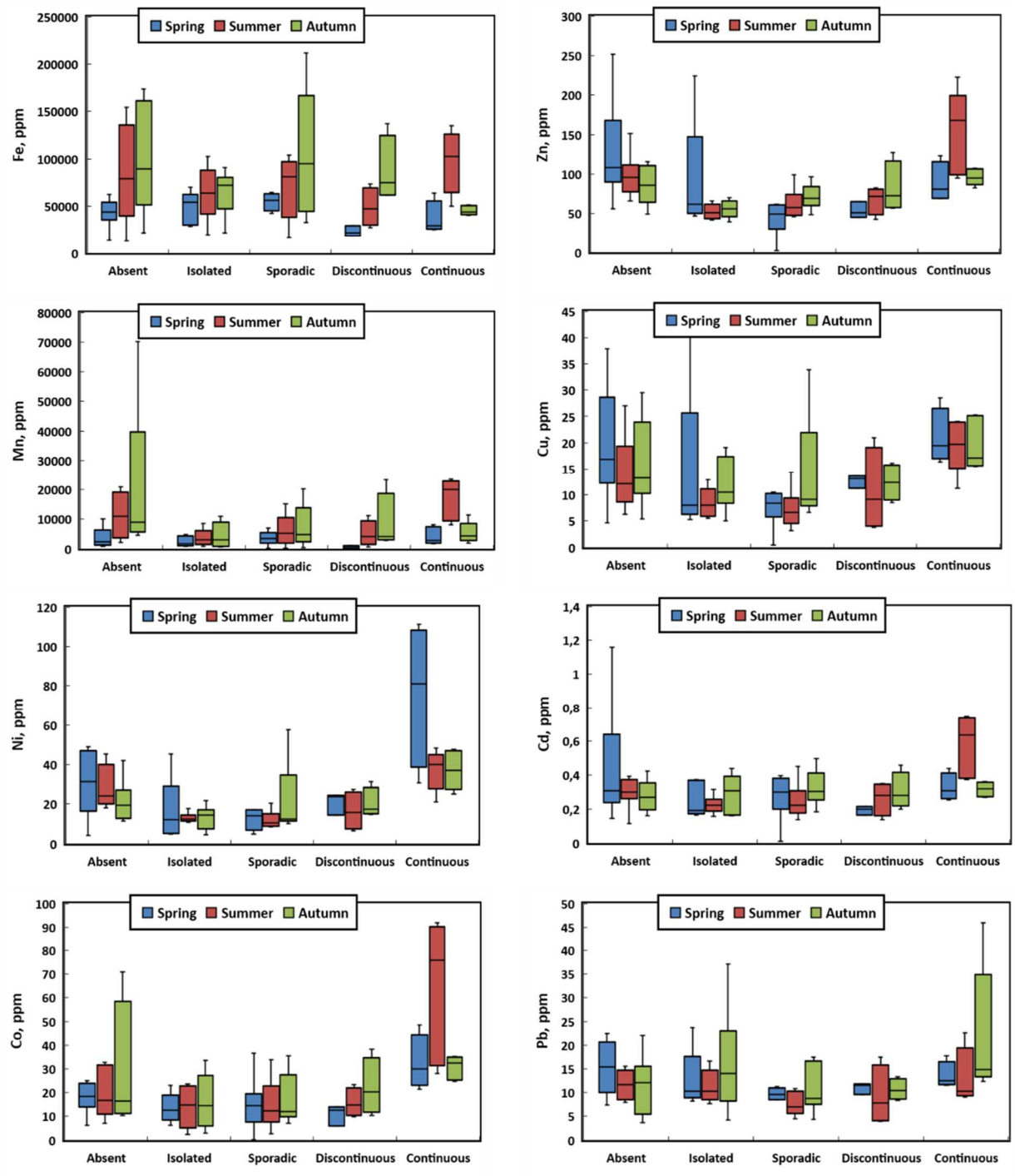

Fig 2, continued

1013 **4th group & 5th group**

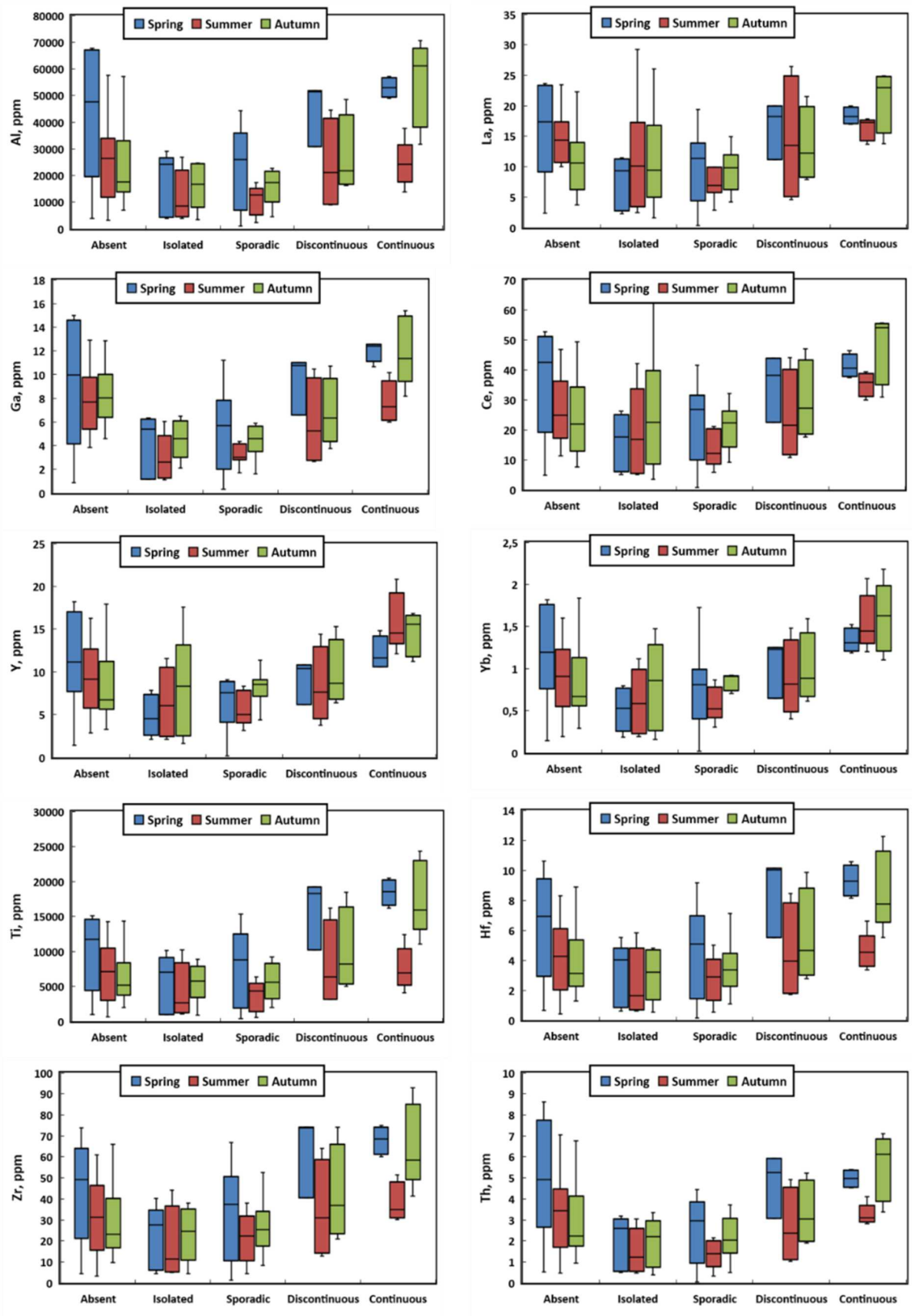

1014

1015

1016 **Fig 2,** continued

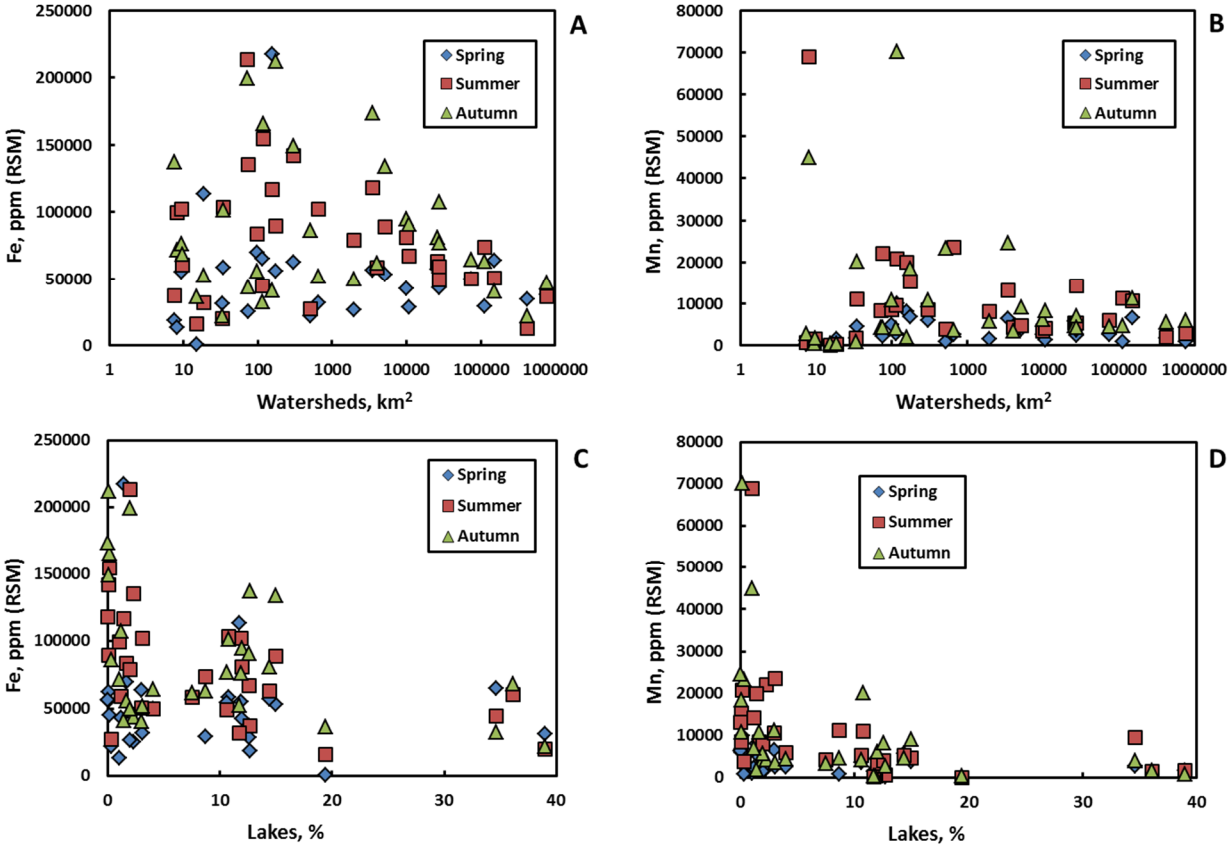

Fig 3. Concentration of Fe (A) and Mn (B) in suspended matter of western Siebrian rivers as a function of watershed area and as a function of lake coverage of the watershed (C, D, respectively). The solid lines represent empirical, 2nd order polynom fit to the concentration dependence on lake percentage, with significant ($p < 0.05$) regression coefficients given in the graphs.

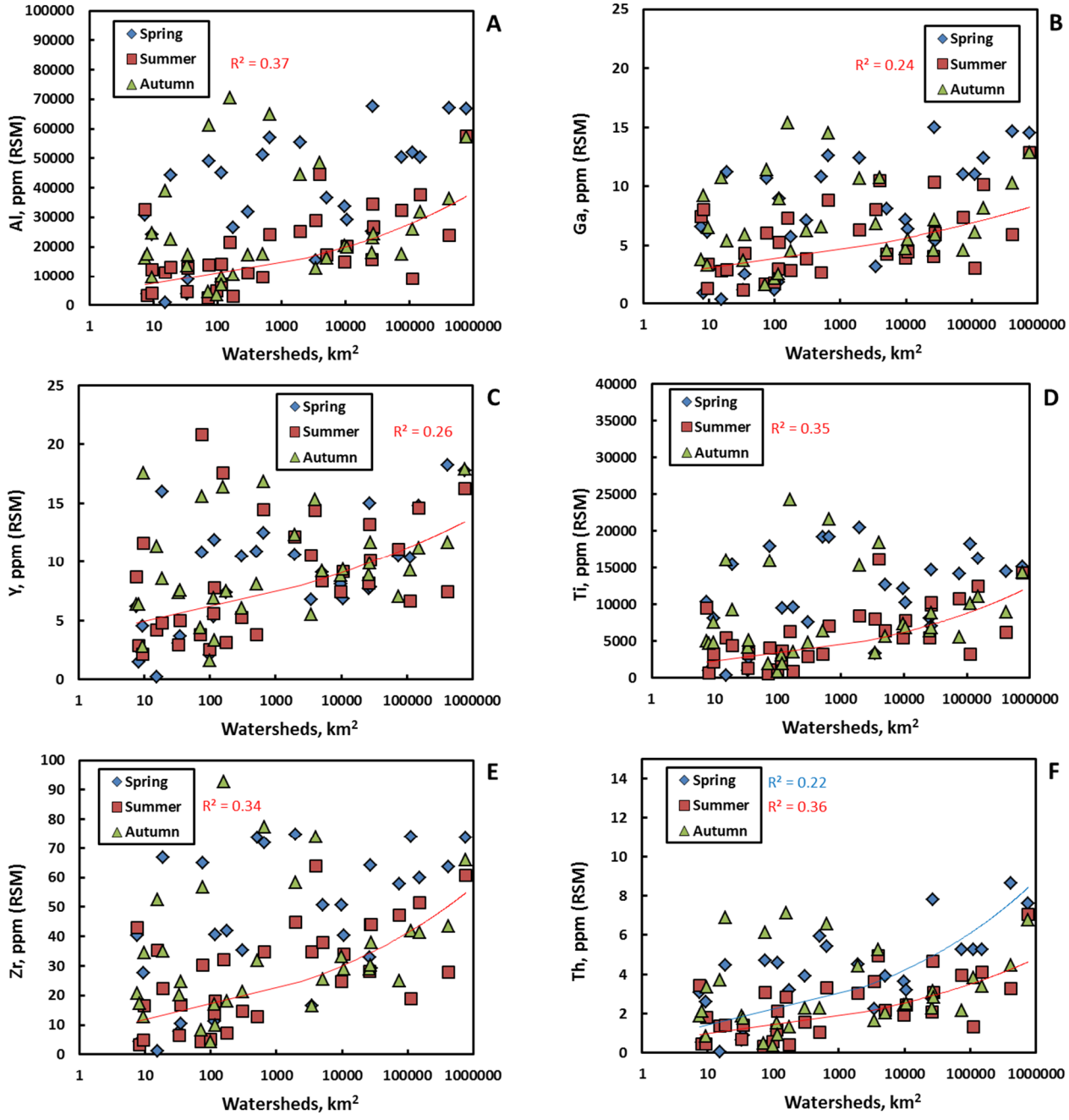

Fig 4. Concentration of Al (A), Ga (B), Y (C), Ti (D), Zr (E) and Th (F) in RSM of WSL as a function of watershed area. The solid lines represent empirical exponential fit to the concentration - watershed dependence with significant ($p < 0.05$) regression coefficients given in the graphs.

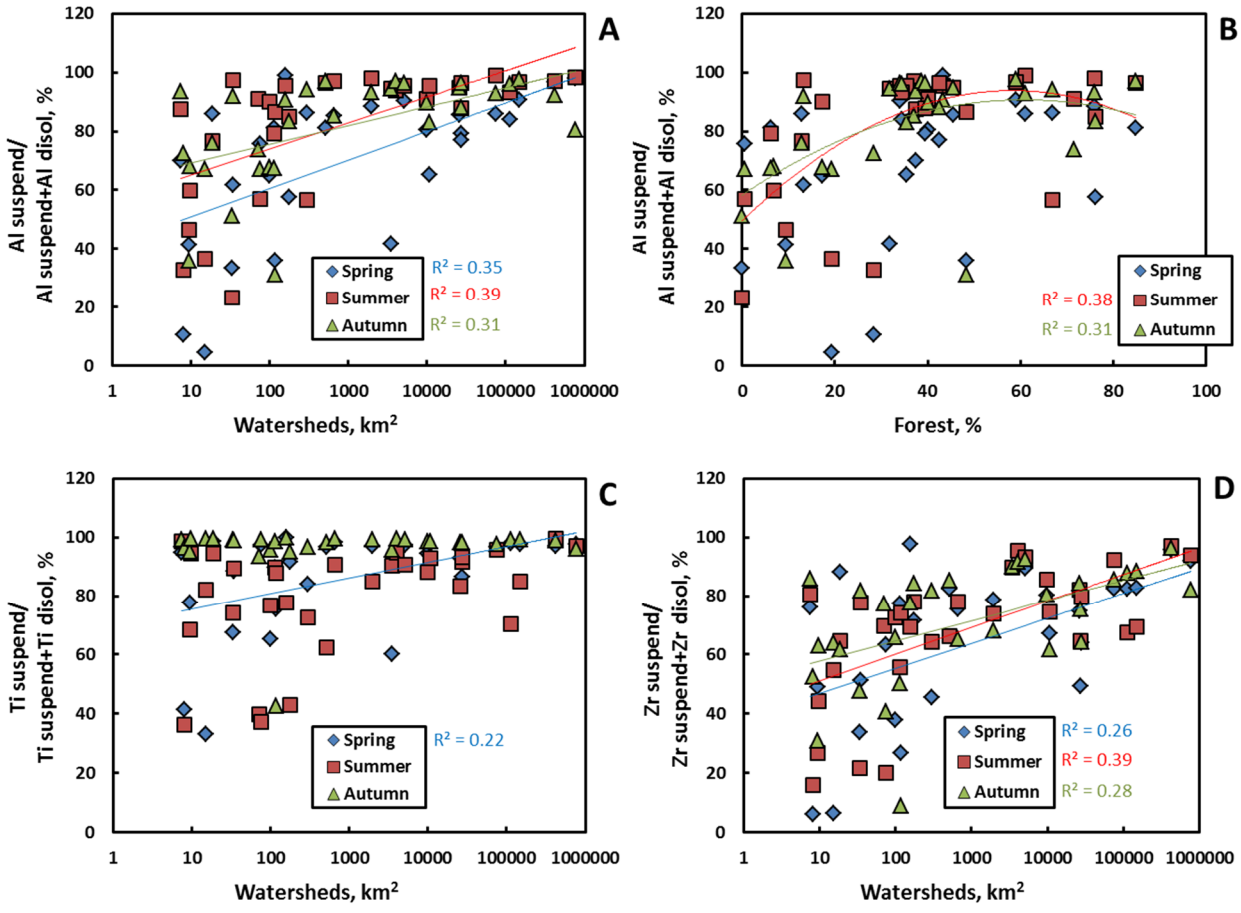

Fig. 5. Suspended fraction of Al in RSM total (suspended + dissolved) transport as a function of watershed area (A) and forest coverage of the watershed (B) and particulate fraction of Ti (C) and Zr (D) as a function of $S_{watershed}$. The solid lines represent 1st or 2nd polynomic empirical fit to the data, with significant ($p < 0.05$) regression coefficients given in the graph.

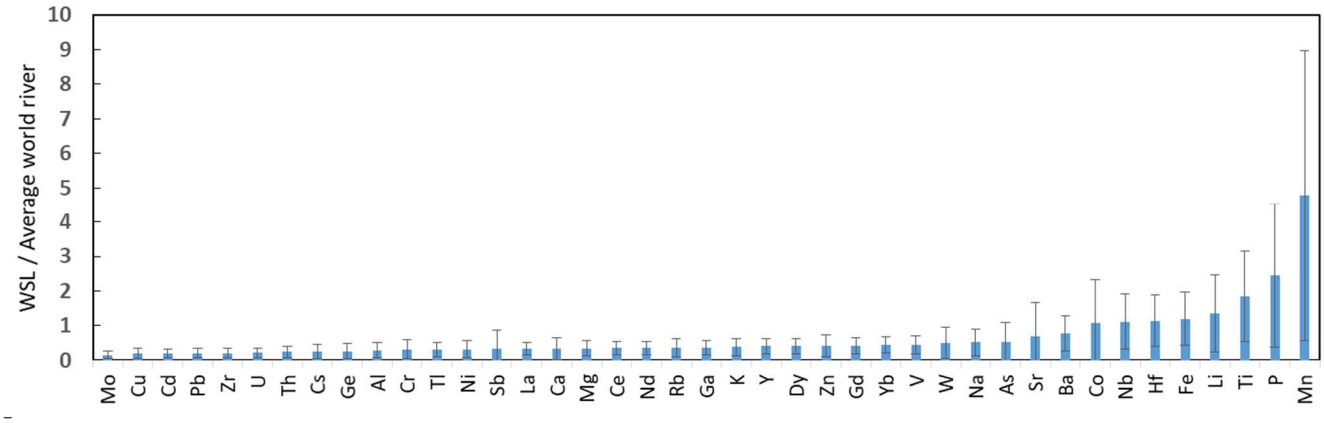

Fig. 6. The ratio of element concentration in RSM of WSL rivers (averaged over all seasons and permafrost zones) to the average element concentration in RSM of rivers worldwide (Viers et al., 2009).

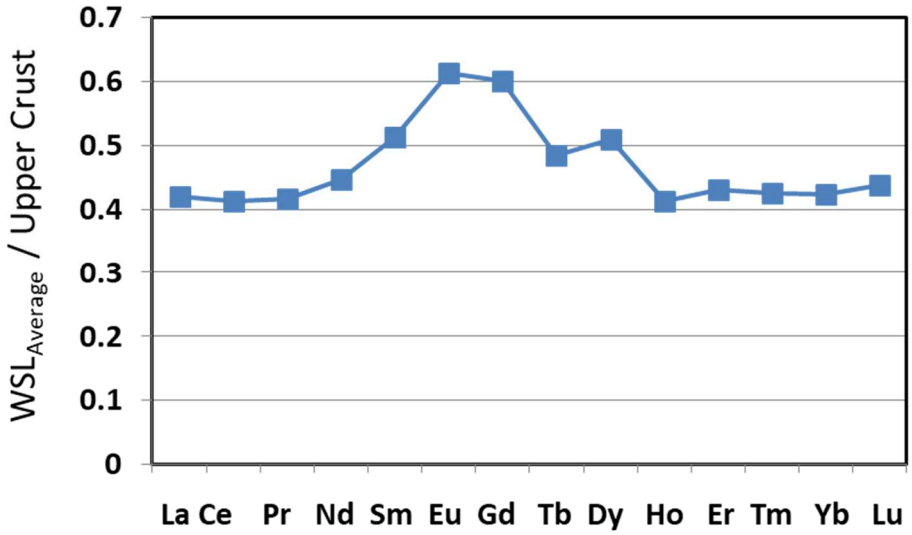

1075

1076

1077 **Fig. 7.** Upper-crust normalized pattern of WSL rivers suspended load (averaged over all seasons,
1078 river sizes and permafrost zones)

1079

1080

1081

1082

1083

1084

1085

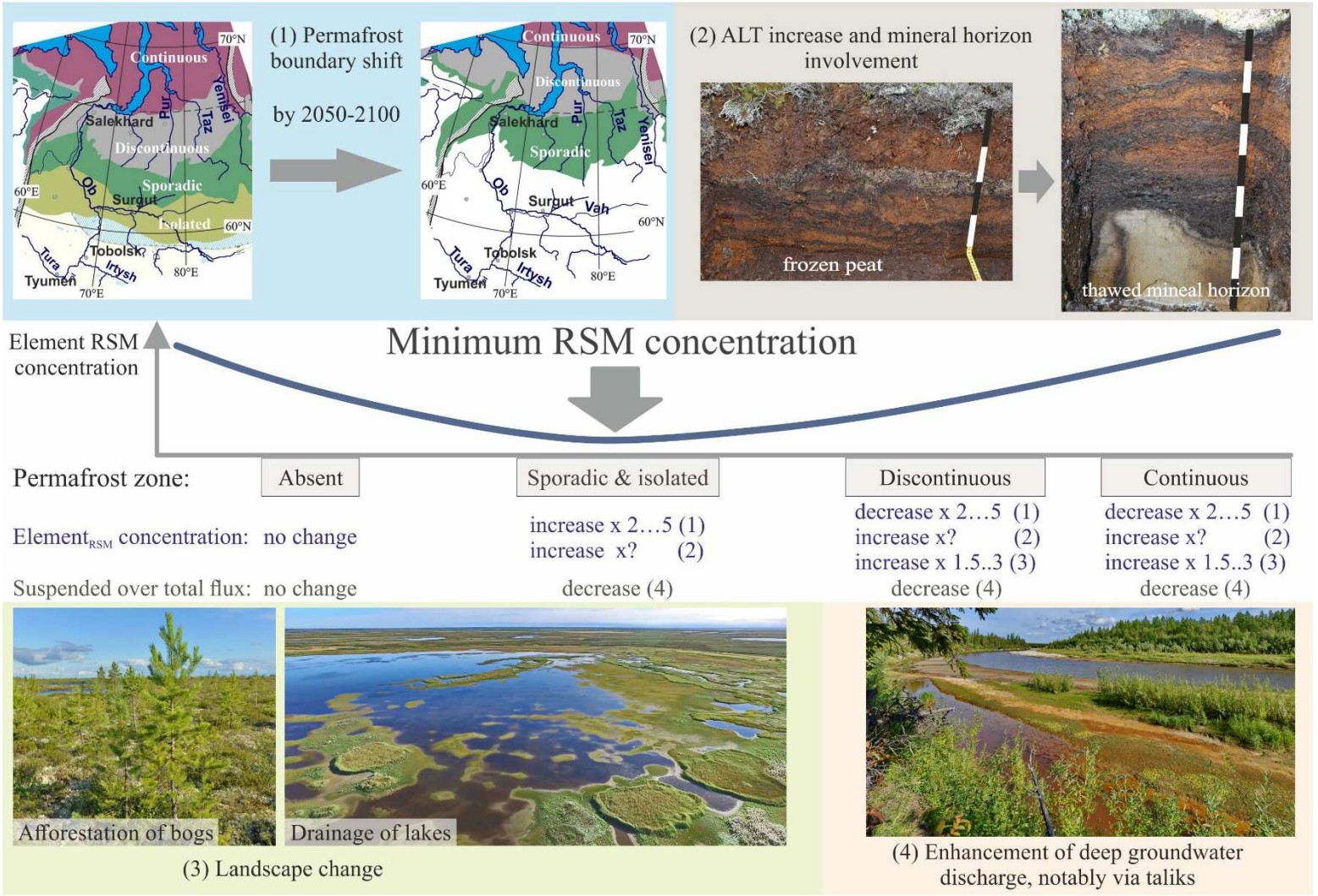

Figure 8. A scheme of element mobilization from the soil to the river in the form of suspended particles and provision for the change of element concentrations in RSM and the share of suspended over total element transport under scenario of climate warming, permafrost thaw and landscape evolution in western Siberia. The 4 relevant processes controlling the RSM delivery from the soil to the river are influenced by climate change in WSL and impact element concentrations in WSL and the share of suspended fraction.

1091 **Table 1.** Mean (± SD) concentrations (ppm dry weight) of elements in RSM of WSL averaged over
1092 all seasons and permafrost zones.

	All seasons	All seasons	All seasons
	permafrost-free N=24	permafrost-bearing N=68	All WSL N=92
Li	15.6±10.7	10.2±8.62	11.6±9.46
B	9.76±8.42	12.4±14.0	11.7±12.8
Na	3713±2284	3760±2856	3748±2707
Mg	5481±2846	4059±2719	4430±2808
Al	30930±20812	24091±17354	25875±18450
P	7007±6047	4187±3004	4923±4176
K	6995±4539	6304±4189	6484±4269
Ca	17097±12323	6048±2917	8930±8273
Ti	7756±4773	8237±6058	8112±5729
V	61.4±31.8	56.6±34.6	57.9±33.8
Cr	42.7±25.3	41.1±34.4	41.5±32.2
Mn	14219±19572	5829±5909	8018±11670
Fe	75641±50000	67760±42800	69816±44700
Co	32.7±44.2	21.8±18.2	24.6±27.6
Ni	26.9±12.8	23.1±20.4	24.1±18.7
Cu	16.4±8.71	14.0±12.3	14.6±11.5
Zn	112.8±58.7	82.1±65.6	90.1±65.0
Ga	8.46±3.74	6.01±3.63	6.65±3.80
Ge	0.42±0.30	0.30±0.25	0.33±0.27
As	34.8±28.7	13.9±12.0	19.3±20.0
Rb	36.3±24.3	26.1±18.9	28.8±20.8
Sr	180±117	115±193	132±178
Y	9.75±4.85	8.75±4.56	9.01±4.63
Zr	34.8±21.2	34.5±22.1	34.6±21.7
Nb	15.7±9.69	14.9±11.1	15.1±10.7
Mo	0.49±0.43	0.45±0.31	0.46±0.34
Cd	0.35±0.22	0.31±0.19	0.32±0.19
Sb	0.73±0.57	0.71±1.33	0.72±1.17
Cs	2.40±1.74	1.39±1.04	1.65±1.33
Ba	617±357	329 ±181	404±270
La	13.9±6.29	12.2±6.80	12.6±6.68
Ce	28.9±15.0	25.5±14.6	26.4±14.7
Pr	3.20±1.68	2.88±1.65	2.96±1.66
Nd	12.4±6.46	11.3±6.37	11.6±6.37
Sm	2.53±1.31	2.24±1.23	2.31±1.25
Eu	0.59±0.27	0.52±0.28	0.54±0.28
Gd	2.50±1.25	2.20±1.20	2.28±1.21

Tb	0.34±0.17	0.30±0.16	0.31±0.17
Dy	1.92±0.99	1.73±0.94	1.78±0.95
Ho	0.36±0.18	0.33±0.17	0.33±0.18
Er	1.06±0.55	0.97±0.51	0.99±0.52
Tm	0.15±0.08	0.14±0.07	0.14±0.07
Yb	0.97±0.51	0.91±0.48	0.93±0.49
Lu	0.14±0.07	0.13±0.07	0.14±0.07
Hf	4.80±3.01	4.57±2.99	4.63±2.98
Ta	1.17±0.73	1.04±0.77	1.07±0.76
W	0.95±0.48	1.04±2.24	1.02±1.94
Tl	0.20±0.13	0.16±0.10	0.17±0.11
Pb	12.8±5.22	12.9±9.00	12.8±8.16
Th	3.78±2.38	2.75±1.77	3.02±1.98
U	0.81±0.49	0.68±0.42	0.72±0.44

Table 2. The percentage of particulate (> 0.45 μm) over total (particulate + dissolved (< 0.45 μm)) concentration of elements in WSL rivers across three seasons and two permafrost zones (mean ± SD).

	Spring		Summer		Autumn	
	permafrost-free N=8	permafrost-bearing N=20	permafrost-free N=8	permafrost-bearing N=24	permafrost-free N=8	permafrost-bearing N=24
Li	8.76±8.69	11.3±8.4	4.45±3.08	2.45±2.36	1.20±0.77	5.22±4.61
B	0.61±0.55	1.89±1.12	0.55±0.55	0.71±0.94	0.10±0.09	2.17±2.67
Na	1.54±1.41	3.59±3.34	0.73±0.65	1.49±3.20	0.14±0.13	1.67±2.06
Mg	2.09±2.22	4.04±3.93	0.72±0.59	3.08±5.34	0.19±0.16	3.83±5.97
Al	66.8±32.8	70.2±22.0	81.6±24.0	82.2±21.4	81.8±22.1	81.3±16.1
K	6.44±6.19	19.8±14.2	6.19±5.54	8.17±9.39	1.47±1.48	15.8±14.8
Ca	0.46±0.46	2.61±2.47	0.41±0.21	1.52±1.76	0.17±0.13	2.08±2.37
Ti	79.9±20.1	88.1±16.2	83.9±21.0	79.3±17.8	90.3±19.2	98.4±1.68
V	42.7±26.8	54.3±17.2	45.3±19.0	48.3±19.4	27.1±18.7	54.1±16.1
Cr	49.8±34.6	32.5±21.3	59.1±22.8	51.4±21.2	29.9±17.2	36.8±14.4
Mn	59.8±19.6	32.9±21.7	83.8±21.8	56.0±36.0	93.8±10.0	46.5±27.8
Fe	49.4±28.5	51.3±18.5	79.1±21.0	71.1±23.3	71.1±19.6	72.8±17.6
Co	53.2±25.0	42.3±22.1	64.2±17.2	48.3±21.5	42.6±24.1	47.6±20.2
Ni	16.3±17.5	16.3±11.0	25.4±22.5	24.8±21.8	8.37±5.06	25.4±14.0
Cu	8.41±7.71	20.5±11.8	22.2±15.1	24.2±16.1	17.4±16.7	39.0±19.6
Zn	23.0±19.2	15.2±10.8	50.3±17.2	26.9±14.7	36.9±23.1	38.5±14.5
Ga	81.0±20.8	75.4±20.5	85.9±9.5	76.6±22.0	76.2±19.6	80.0±15.9
As	10.6±7.4	14.3±8.2	25.9±16.7	19.3±10.5	19.6±18.2	26.9±12.9
Rb	30.0±26.5	34.5±20.9	24.3±18.7	16.8±13.3	7.34±4.32	30.7±20.1
Sr	1.13±1.34	7.01±6.11	0.90±0.52	2.68±2.58	0.33±0.27	4.13±4.06
Y	31.6±28.7	29.6±17.7	68.8±22.5	48.6±17.7	52.2±23.8	48.3±18.4
Zr	52.9±33.7	66.6±21.2	74.0±27.0	66.7±20.4	71.6±28.4	70. 8±16.7
Nb	77.5±26.4	89.6±15.8	87.0±20.9	90.2±10.7	84.5±26.4	95 6±5.8
Mo	1.64±1.07	22.5±17.8	4.29±3.8	17.5±15.7	2.07±2.73	27.6±19.3
Cd	19.8±11.8	22.3±13.5	41.5±26.7	28.1±19.0	32.7±19.1	44.4±21.5
Sb	6.35±4.19	12.0±9.54	9.51±6.5	13.1±10.6	13.4±11.7	23.6±16.7
Cs	76.2±28.4	72.5±30.1	80.8±26.8	60.8±25.9	68.8±27.1	71.2±26.0
Ba	11.6±9.08	31.0±20.1	15.7±6.7	24.8±14.3	6.95±5.27	28.1±17.4
La	39.4±31.0	34.1±18.8	83.4±17.4	60.4±22.2	73.1±27.6	55.5±22.2
Ce	47.3±30.9	42.6±18.9	87.4±18.4	66.9±21.6	82.0±24.5	67.1±20.1
Nd	39.6±32.0	39.2±18.3	80.2±23.8	61.6±21.4	74.5±25.2	61.6±20.8
Yb	31.8±29.6	30.2±15.8	65.7±24.4	44.1±17.5	53.0±25.6	43.3±16.1
Hf	54.8±33.8	64.5±21.5	77.3±25.1	66.6±22.9	74.2±28.1	76.5±15.5
Pb	54.6±29.6	57.8±24.0	85.0±14.1	56.3±21.8	79.8±22.6	79.8±11.4
Th	50.1±34.6	57.5±18.9	84.6±25.1	66.6±19.6	84.1±20.7	67.6±17.2
U	9.84±13.2	43.0±17.7	10.9±16.5	43.0±22.9	6.60±9.52	51.8±18.5